Spike-based Learning Rules and Stabilization of Persistent Neural Activity

by

Xiaohui Xie

Submitted to the Department of Electrical Engineering and Computer Science
in partial fulfillment of the requirements for the degree of

Master of Science in Computer Science and Engineering

at the

MASSACHUSETTS INSTITUTE OF TECHNOLOGY

August 2000
[September 2000]

Author .....
Department of Electrical Engineering and Computer Science
August 6, 2000

Certified by .....
H. Sebastian Seung
Assistant Professor
Thesis Supervisor

Accepted by .....
Arthur C. Smith
Chairman, Department Committee on Graduate Students

Spike-based Learning Rules and Stabilization of Persistent Neural Activity

by

Xiaohui Xie

Submitted to the Department of Electrical Engineering and Computer Science
on August 6, 2000, in partial fulfillment of the
requirements for the degree of
Master of Science in Computer Science and Engineering

Abstract

In this thesis, I studied the biophysically plausible mechanism for the function of neural integrator, a premotor area responsible for controlling eye movement. A transient input to the integrator neurons can cause the persistent change of their neural activities. The exact mechanism underlying the function of the neural integrator still remains largely unknown. In this thesis, I used a biophysically realistic recurrent neural network to model the integrator function. The spike-based learning rules are implemented in the network as an internal adaptive mechanism for stabilizing persistent neural activities.

Thesis Supervisor: H. Sebastian Seung
Title: Assistant Professor

Acknowledgments

I am most grateful to Prof. Sebastian Seung for his constant guidance and encouragement. I also would like to thank Dr. Richard Hahnloser for his advise and helpful discussions. Special thanks also goes to other members of Seung lab, who have helped this work in one way or another.

Contents

Chapter 1

Introduction

In a wide range of areas have been observed the persistent change of the neural activities after a transient stimuli is presented. Such step change of neural activities can sustain up to many seconds, and is called *persistent neural activity* in many literatures [1, 2, 3]. The persistent neural activity is generally thought to be the neural basis of the *short term memory* and carries the information temporarily about the transient stimuli presented.

The physiology of the short term memory has been intensively studied in several areas, such as the prefrontal cortex, the limbic system and the occulomotor integrator[4, 5, 6]. Extracelluar recordings of the neural activities show that neurons in these areas are able to maintain a persistent activities in a variety of behavioral tasks, even though the contents of the short term memory are significantly different from each other.

The exact mechanism for the neural system to maintain a persistent neural activity still remains unclear. Recently there has been a booming of interest in this area and many models have been proposed. The predictions from models have been studied and tested in the carefully designed experiments. Although some of the predictions have been observed in the experiments, all models share some aspects of disadvantages. Later in this chapter, we will review briefly some of the models.

Oculomotor neural integrator serves a good example system for studying the persistent neural activity [2, 7, 1]. A transient saccadic input from command neurons

will cause an elevated or suppressed discharge of the integrator neural activity. The step change of this activity can sustain for many seconds and stores a short term memory of the eye position. It is called integrator in the sense that the transient input is integrated into a persistent step signal. Integration of the saccadic burst input is only one aspect of the integrator function. In the vestibular-occulo-reflex(VOR), the integrator is able to integrate the head velocity signals into the position signals.

In this thesis, we study the mechanism of the short term memory in the oculomotor neural integrator. Although the mechanisms of short term memory are unlikely to be exactly the same among different systems, they might share some similar principles. The goal of this thesis is to understand the mechanism of the persistent neural activity in the oculomotor integrator and gain some insight about the mechanism of short term memory in general.

1.1 Oculomotor neural integrator

The oculomotor neural integrator stores a short term memory of the eye position. In the mammals, it has been localized in at least two nuclei of the brain stem – propositus hypoglossi(PH) and the medial vestibular nucleus (MVN)[8]. These two nuclei store and maintain the short term memory rather that just acting as a relay station. This has been shown in several different types of experimental studies: single unit recording, micro-stimulation and pharmacological inactivation. It has been shown that micro-stimulation of the integrator neurons causes the movement of the eye position and pharmacological inactivation leads to the drift of eye position[9, 10]. In goldfish, the localization of the integrator was first done in Baker's lab [11, 12]. It has been localized to the Area I of the goldfish brain stem.

The oculomotor neural integrator receives input from several nuclei commanding different types of eye movements. For example, it receives input from burst neurons for the saccadic eye movement and vestibular neurons for VOR. The integrator neurons send the output to the extraocular motor neurons, which act as a plant for controlling the eye movement.

It has been observed widely in the experiments that the firing rate of the integrator neuron is roughly a linear function of the angular eye position. In the saccadic eye movement, a transient burst neuron input will cause persistent step changes in the integrator neural activity and hence the movement of the eye position. Because the close relationship between the integrator neuron activity and the precise eye position, to keep the eye still the neural activity of the integrator neurons has to be maintained consistently. The time domain after each saccade is called *gaze-holding period.* The mechanism for the neural integrator to hold persistent activity during gaze-holding period is the subject of this thesis and will be studied intensively in later chapters.

1.2 Mechanism of short term memory

Depending upon which level it is acting on, a model can be basically classified into two categories – cellular or circuit model. People in cellular modeling argue that the persistent neural activity is caused by cellular mechanism such as synaptic plasticity or cell membrane properties [13, 14, 15, 16]. The synaptic facilitation in the retinotectal synapse has been proposed as the mechanism for neuron in the tectum of frog to keep a short term memory of the visual images[16]. Other models utilize the properties of the membrane bistability to store the short term memory. For example, due to the bistability in spinal motor neuron, stimulation of the proprioceptive afferent can lead to persistent change in the spinal motor neuron activities, which is proposed as a short term memory of the posture[15]. Lisman et al proposed a model based on the bistability of the NMDA receptor to explain the short term memory in the prefrontal cortex[14].

On the other hand, people in the circuit modeling argue that it is the recurrent network that is being used to store the short term memory. This idea is first proposed by Lorente de No[17]. He proposed the reverberations in feedback loops of a recurrent network as the mechanism of the short term memory.

To model the oculomotor neural integrator, Robinson et al took a circuit approach and implemented the reverberation in a linear recurrent network model[3, 7].

Robinson's linear feedback model makes a lot of progress and many predictions from the model have been observed in the experiments. First, since the model is linear, it explains well the linear relationship between integrator neural activities and the eye position. Second, the persistent neural activities degrade with the extent of the mistuning of the synaptic weights, which has also been observed in experiments by using pharmacological inactivation techniques. Third, the model predicts that the relationship between drift velocity and eye position should be linear. This has also been observed in some mammals.

Despite the great success, the linear feedback model has several unfavorable features. First, it uses a continuous variables to describe the neural activities, but real neurons fire action potentials. Second, the activity of the biophysical neuron is highly nonlinear. It fires only above certain threshold and saturates at high firing rate. A linear model ignores these properties. As a result, the linear feedback model predicts a linear relationship between the drift velocity and eye position. Though it holds in some experiments in certain animals, recently more precise measurement in goldfish shows that this relationship is actually nonlinear.

A significant progress has been made recently by Seung et al[1], who build a biophysically realistic conductance-based model as the mechanism of short term memory in the oculomotor neural integrator. The model predicts the linear relationship between integrator neural activity and eye position and also the degradation of the persistent neural activity with the mistuning of the synaptic weights just as in linear feedback model. However, because the model considers the threshold and saturation nonlinearity, it predicts that the drift velocity should be a nonlinear function of the eye position, which is consistent with more precise measurement of the drift velocity in goldfish.

1.3 Continuous attractor is used to store the analog memory

A hypothesis first proposed by Amit is that the persistent neural activities is identified as the fixed points of the dynamics system [18]. Different levels of the persistent activities are corresponded to different fixed points. Whether this hypothesis is valid is still unclear, although most of the recurrent network models utilize this idea. In Seung's model, the eye positions are stored approximately as a line attractor, which is a continuous manifold of the fixed points.

Line attractor is suited for storing the continuous variables such as the eye position in the oculomotor integrator, orientation in the visual cortex neurons and head direction cells in the limbic system. Not all short term memories should be identified as continuous attractors. For example, the short term memories in the prefrontal cortex are discrete, and thus are the scattered fixed points in the state space.

The hypothesis for the identification of short term memories as the fixed points are critical in most of the models we have discussed, which plays an important role not only in the short term memory model, but also in a variety of other models such as the Hopfield network which stores the associate memories as the fixed points of the dynamics systems[19, 20].

1.4 Criticism: precise tuning

For the feedback network to keep persistent activity, the weights of the recurrent network have to be precisely tuned. This is the case in both Robinson's linear feedback model and Seung's conductance-based recurrent network model. We will illustrate this in a linear model $\tau\dot{x} + x = wx + b$. The time constant of this model is $T = \tau/(1-w)$. If $\tau = 100$ ms and the integrator time constant T need to be 10 seconds, the synapse weight w has to be precisely 0.99. A variation of w with 1% will cause the model to be unstable or with a time constant less than 5 seconds. Thus precisely tuned model does not seem to be robust.

Thus for the recurrent network model to work, at least two critical issues have to be addressed. First, how does the neural network tune itself? Second, if the weights are mistuned, what kind of adaptive mechanism could be utilized to recover the tuned values?

We conclude these questions as a learning problem. Next we will show what kind of information and learning rules could be used in this challenging learning process.

1.5 Learn to tune the synaptic weights

Sensory information such as the visual and proprioceptive feedback could be very important for the learning process. For example, the mismatch between the desired eye position and actual one coming from visual feedback could provide important information for the neural system to change the synaptic weights. Robinson et al takes this information for the learning of synaptic weights in their linear feedback network[21].

However, recent experimental results show that rat raised in the dark environment since born can still learn VOR[22]. Another evidence is the experiment on goldfish done in Tank's lab. After the integrator is trained to be leaky, the animal is kept in a dark environment lack of sensory feedback. The preliminary result show that the animal can still learn to hold still gaze.

These experimental evidences show that besides the sensory feedback there must exist other internal mechanisms for the neural integator to learn to tune the synaptic weights such that the persistent neural activity could be maintained. The learning rule based on the internal information rather than external sensory feedback is the one we will explore in the later chapters.

The learning rule we will implement is based on spike relationship of the biophysical neurons. The spike based learning rules play an important role in a variety of neural systems. Recently significant progresses have been made in our understanding of them.

Hebb probably is the first one who proposed a learning rule based upon the action

potentials of the neurons. The so called *Hebbian learning rule* states that the synaptic weight increases when the pre and post synaptic neurons fire spike simultaneously, or in simple words: "Neurons firing together wire together"[23].

However, Hebbian learning rule is not the only one that has been observed in the neural systems. Recently, people have discovered another types of learning rules depending critically on the temporal differences between pre and post synaptic spikes. According to this rule, a synapse depresses when a presynaptic spike is followed by a postsynaptic spike, and potentates when the order is reversed. This type of *differential anti-Hebbian* dependence on temporal order has been observed in electrosensory lobe synapses of the electric fish [24], but is opposite to the *differential Hebbian* dependence observed at cortical [25] and hippocampal synapses[26].

If the function relating synaptic change to the temporal difference between presynaptic and postsynaptic spikes is antisymmetric, then neural activity at constant firing rates results in no net change in synaptic strength, provided that the cross-correlogram of the spike trains is symmetric about zero.

Therefore changes in firing rate are required to induce synaptic plasticity. More specifically, we will show later that anti-Hebbian learning based on spike times is equivalent to changing the strength of a synapse by the product of the presynaptic firing rate and the time derivative of the postsynaptic firing rate, with a minus sign.

In effect, this synaptic learning rule uses a negative feedback signal to reduce drift in neural activity. We have applied the learning rule to stabilize persistent neural activity in a recurrent network model of the oculomotor velocity-to-position integrator. The learning rule is applied during the time intervals between saccadic burst inputs, reducing the drift in firing rates by tuning the strength of synaptic feedback continuously.

Chapter 2

Spiking neurons and recurrent network model

Spiking neuron in this thesis is described by the *integrate-and-fire* model. The integrate-and-fire model is a simplification of the detailed conductance-based model, however it still keeps some essential biophysical properties. Because of the simplification, the integrate-and-fire model could be subjected to many analytical analysis. In this chapter, we will describe several important properties of the integrate-and-fire model, such as the relationship between the firing rate and the applied current or synaptic conductance, which will be used in later chapters.

A recurrent network describes a population of the integrate-and-fire neurons forming synaptic connections from each other. We will show how to reduce the spiking neural models to the traditional continuous network model by using the method of averaging under certain conditions. The reduced Wilson-Cowan form network equations play a critical role in our analysis in later chapters when we study the tuning and learning problems[27, 28].

2.1 Integrate-and-fire neuron

2.1.1 Basic definition

The integrate-and-fire model is a simplified description of the biophysical spiking neuron. When the applied current is over some threshold, the membrane potential will exponentially increase. After hitting the action potential threshold, a action potential will be produced and the membrane potential is reset to resting voltage.

The change of the membrane potential can be described by the following dynamic equation.

$$C_m \frac{dV}{dt} = I_L + I_{syn} + I_{app} \tag{2.1}$$

$$I_L = -g_L(V - V_L) \tag{2.2}$$

$$I_{syn} = -g_{syn}(V - V_{syn}) \tag{2.3}$$

where V is the membrane potential, C_m the capacity, g_L the leak conductance and g_{syn} the synaptic conductance. V_L and V_{syn} are equilibrium potentials of leak conductance and synaptic conductance respectively.

We will denote the action potential threshold by V_{th}, and the resting potential by V_0. To simplify the model, here we did not consider the refractory time period after the firing of the action potential.

The parameters used in the model is listed in table (2.1.1)[29].

C_m	0.5 nF
g_L	0.025 μs
V_L	-70 mv
V_{th}	-52 mv
V_0	-59 mv

Table 2.1: Biophysical parameters of the integrate-and-fire neuron

2.1.2 Current threshold

The integrate-and-fire model can be reformulated as

$$\frac{dV}{dt} = -\frac{g_L}{C_m}V + \frac{g_L V_L + I_{syn} + I_{app}}{C_m} \tag{2.4}$$

After each action potential, the membrane potential is reset to the resting potential V_0 and will exponentially increase. The solution of this equation after each action potential is described by:

$$V = (V_0 - \frac{g_L V_L + I_{syn} + I_{app}}{g_L})e^{-g_L/C_m t} + \frac{g_L V_L + I_{syn} + I_{app}}{g_L} \tag{2.5}$$

The equilibrium point of the above solution is $(g_L V_L + I_{syn} + I_{app})/g_L$. For the potential V to be able to reach the firing threshold, the sum of synaptic and externally applied current $I_{syn} + I_{app}$ must be larger than the current threshold:

$$I_c = g_L(V_{th} - V_L) = 0.45nA \tag{2.6}$$

Also from the solution of V, we can see that the time constant of the action potential is $\tau_m = C_m/g_L = 20ms$.

2.1.3 Firing rate of integrate-and-fire neuron

Typically the activity of a neuron is described by the firing rate of action potentials. In this section, we will calculate the firing rate as a function of the externally applied current I_{app} and as a function of the synaptic conductance g_{syn}. In both cases, we will show that when I_{app} or g_{syn} is large enough, the firing rate could be approximated by a linear function of I_{app} or g_{syn} respectively.

First we will discuss the case when the synaptic current I_{syn} is zero and a constant current I_{app} larger than the threshold current I_c is applied. In this case, the neuron

will fire repetitively with a constant period. The firing rate is determined by:

$$\nu = \frac{g_L}{C_m ln(1 + \frac{g_L(V_{th}-V_0)}{I_{app}+g_L(V_L-V_{th})})} \tag{2.7}$$

This is a highly nonlinear function. However, when I_{app} is large, i.e. $I_{app} >> g_L(V_{th} - V_0) - g_L(V_L - V_{th})$, the firing can be approximated as a linear function of the applied current.

$$\nu \approx \frac{1}{C_m(V_{th} - V_0)} I_{app} + \frac{g_L(V_L - V_{th})}{C_m(V_{th} - V_0)} \tag{2.8}$$

Next we will analyze the firing rate as a function of the synaptic conductance g_{syn} when the externally applied current is zero. Again in this case, neuron will fire with a constant firing rate. By using Eq. (2.5), the rate is determined by the following equation.

$$\nu(g_{syn}) = \frac{g_L + g_{syn}}{C_m} [ln \frac{(V_0 - V_{syn})g_{syn} + (V_0 - V_L)g_L}{V_{th} - V_{syn})g_{syn} + (V_{th} - V_L)g_L}]^{-1} \tag{2.9}$$

Again, we will consider the case when g_{syn} is large. In this case the firing rate can also be approximated as a linear function of g_{syn}.

$$\nu(g_{syn}) \approx a g_{syn} + b \tag{2.10}$$

$$a = \frac{1}{C_m ln((V_0 - V_{syn})/(V_{th} - V_{syn}))} \tag{2.11}$$

$$b = g_L \frac{1 - (\frac{V_0 - V_L}{V_0 - V_{syn}} - \frac{V_{th} - V_L}{V_{th} - V_{syn}})[ln((V_0 - V_{syn})/(V_{th} - V_{syn}))]^{-1}}{C_m ln((V_0 - V_{syn})/(V_{th} - V_{syn}))} \tag{2.12}$$

2.2 Recurrent network of spiking neurons

The recurrent network is comprised of a population of integrate-and-fire neurons forming synaptic connections with each other. These synaptic connections contribute the the synaptic conductance g_{syn} and thus change the synaptic current. The contribution of synaptic conductance from presynaptic to postsynaptic neuron is determined by

two major factors. The first one is the synaptic strength between these two neurons. The second factor is the activity of the presynaptic neuron, which determines how many neurotransmitter will be released and thus the channel activity of the postsynaptic neuron. We will denote the second variable by s and call it the *channel variable* although its direct connection is the concentration of the released neural transmitter.

The variable s is a dynamical variable with close relationship to the presynaptic membrane potential since the release of neurotransmitter is usually triggered by the depolarization of the presynaptic neuron. Moreover, the dynamics is also determined by the type of the ligand-gated channels in the postsynaptic membrane. Thus biophysically the channel variable should be determined by both pre and post synaptic neurons. However, in our model we will simplify the description and assume the post synaptic channel is gated by some similar channel, for example N-methyl-D-aspartate(NMDA) receptor[30], and describe the dynamics of the channel variable s purely by the activity of the presynaptic neuron.

2.2.1 Dynamics of channel variables

In this model, all synapses emanating from neuron i to all its targets are described by a variable s_i following the dynamical equations

$$\tau \frac{ds_i}{dt} + s_i = \alpha \sum_a \delta(t - t_{ia}) \tag{2.13}$$

Here, we model the spike trains with the summation of a series of δ function. t_{ia} is the time of the ath spike of this neuron. Spike timing are defined as the voltage resetting times of the integrate-and-fire neurons.

The variable s_i is a characterization of activity of the channels. It is dimensionless and range from zero to one denoting inactive to complete open respectively. Usually, s_i can be thought as the fraction of open channels at the synapse. The dynamics Eq. (2.13) of the channel variable s_i is relatively simple. It says that s_i will exponentially decay when this is no spike and increase instantaneously with a constant value when the spike is coming. Obviously it is a very simple characterization of the biophysical

channel activities, but still it catches some main points and the simplification helps a lot in the mathematical analysis of the model.

2.2.2 A population of integrate-and-fire neurons

In a recurrent network with a population of integrate-and-fire neurons, the neurons form connection with each other through synapses. As we have already mentioned, the contribution to the synaptic conductance $g_{syn,i}$ of neuron i from presynaptic neuron j is determined by the synaptic strength w_{ij} and the channel variable s_j in the form of

$$g_{syn,i} = \sum_{j=1}^{N} w_{ij} s_j \tag{2.14}$$

where N is the total number of neurons in the network.

In summary, a recurrent network of integrate-and-fire neurons are characterized by the following dynamical equations

$$C_m \frac{dV_i}{dt} = -g_L(V_i - V_L) - g_{syn,i}(V_i - V_{syn}) \tag{2.15}$$

$$g_{syn,i} = \sum_j W_{ij} s_j \tag{2.16}$$

$$\tau \frac{ds_j}{dt} + s_j = \alpha \sum_a \delta(t - t_{ja}) \tag{2.17}$$

These set of equations describing the details of spiking-based recurrent network will be the one we used in our simulation. However, the spiking neuron model is not easily suited for mathematical analysis. Next we will take a approximation approach to reduce them to the network model based on continuous variables.

2.2.3 Reduction of the spike-based network to the rate-based one

In the above system equations describing the spiking network model, there have basically two different time scales. One is determined by the dynamical equation of

the membrane potential with a time constant $\tau_m = C_m/g_L = 20ms$. The other one is determined by the channel variable dynamics with a time constant τ.

In the case when the channel variable time constant τ is large, for example, $\tau = 100 \sim 150ms$, the dynamics of s_i is relatively slow compared to membrane potential V_i. Thus we can approximate the right hand side of the channel dynamical Eq. (2.13) with a time average of the fast variable V_i. This results in the following approximation:

$$\begin{aligned} \tau\frac{ds_j}{dt} + s_j &= \alpha\sum_a \delta(t - t_{ja}) && (2.18)\\ &= \frac{1}{T}\int_0^T \alpha\sum_a \delta(t - t_{ja})dt && (2.19)\\ &= \alpha\nu(g_{syn,j}) && (2.20) \end{aligned}$$

The averaging method approximates the spikes trains in the right hand side of channel dynamics Eq. (2.13) with firing rate of this neuron. As a result we have the following closed form equation for slowly changing variable s_i.

$$\tau\frac{ds_j}{dt} + s_j = \alpha\nu(\sum_j W_{ij}s_j) \tag{2.21}$$

This equation is the Wilson-Cowan form of neural network. We will denote the function $\nu(\cdot)$ by $f(\cdot)$ in later chapters and call it *the activation function.*

The reduced rate-based network depends critically on the time constant of the channel variables. If the channel variable is fast, for example the AMPA receptor with a time constant around 5 ms, the time averaging approximation is not good, and this method will fail. However, for the fast channel variable dynamics, when the number of neurons in the network is sufficiently large, spiking models could also be reduced to the continuous variable based model through the way of spatial mean-field approximation rather than the temporal time average.

Chapter 3

Tuned model of oculomotor neural integrator

In this chapter, we will illustrate how positive feedback could be used in the modeling of the short term memory. In particular, we will take the oculomotor neural integrator as an example and show how to tune the weights of the synaptic connections such that the neural activity could be maintained during the gaze holding period.

As we have already introduced in the first chapter, the oculomotor neural integrator is the brain stem premotor nuclei responsive for controlling eye movement and maintaining eye position. In the saccadic eye movement which we will mostly discuss in this chapter, a transient input from the burst command neuron will cause the step change in the activities of integrator neurons, which could sustain for up to many seconds. The integrator neurons project to the motor neurons controlling the extraocular muscle. The integrator neuron is also sometimes called *memory neuron* to emphasize that it stores a short term memory of the eye position. We will mix the use of these two names from now on.

It has been observed that the firing rate of memory neurons is roughly a linear function of the angular eye position. Thus in the recurrent network model of the neural integrator, the synaptic connections in the network must have been constrained in such a way that there is only one degree of freedom in the output of these neurons. In the state space, the fixed points of the network model should only be parametrized

by one parameter, i.e. eye position. Considering the analog feature of the eye position, it is reasonable to argue that the fixed points forming roughly a line in the state space. This observation together with requirement of the persistent activity after each saccade are two immediate tests that every oculomotor neural integrator model has to be examined.

Next we will show the details on how to build the model. We will consider two cases. First an autapse model with localized synaptic feedback will be considered. Second, a distributed recurrent network model is described. The autapse model, though may not biophysically realistic, serves as a good model system for illustrating several main points we will try to explain.

The method used in the chapter is first presented by Seung in his conductance-based model[1]. Here we use a simpler integrate-and-fire model as the basic unit and show how to tune the synaptic weights

3.1 Autapse model

The autapse model is sometimes said to the simplest model possible with feedback. Fig. (3-1) shows the diagram of the autapse model. The core of the circuit is the memory neuron, which makes an excitatory autapse onto itself. It also receives synaptic input from three input neurons: a tonic neuron, an excitatory burst neuron, and an inhibitory burst neuron.

The memory neuron is modeled by the integrate-and-fire neuron and described by the following dynamical equations.

$$C_m \frac{dV}{dt} = -g_L(V - V_L) - g_E(V - V_E) - g_I(V - V_I) \tag{3.1}$$

$$\tau \frac{ds}{dt} + s = \alpha_s \sum_n \delta(t - T_n) \tag{3.2}$$

where g_E and g_I are excitatory and inhibitory synaptic conductances with reversal potentials of $V_E = 0$ mV, and $V_I = -70$ mV respectively. Each spike at time T_n causes a jump in the synaptic activation s of size α_s/τ, where $\alpha_s = 1$, after which s

decays exponentially with time constant $\tau = 100$ ms until the next spike.

The synaptic conductances of the memory neuron are given by

$$g_E = Ws + W_0 s_0 + W_+ s_+ \qquad g_I = W_- s_- \tag{3.3}$$

The term Ws is the recurrent excitation from the autapse, where W is the strength of the autapse. The synaptic activations s_0, s_+, and s_- of the tonic, excitatory burst, and inhibitory burst neurons are governed by equations like (3.1) and (3.2), with a few differences. Each of these neurons has no synaptic input; its firing pattern is instead determined by an applied current.

The tonic neuron has an applied current of 0.49075 nA, which makes it fire repetitively at roughly 30 Hz. Its synaptic time constant is $\tau_0 = 100$ ms. For the excitatory and inhibitory burst neurons the applied current is normally zero, except for brief 50 ms current pulses of 0.95 nA that cause bursts of action potentials. Their synaptic time constants are $\tau_+ = \tau_- = 5$ ms. The excitatory and inhibitory burst synapses have strengths $W_+ = 0.05$ and $W_- = 0.028$.

The question arising here is how to tune the feedback synaptic strength W such that the memory neuron can hold persistent activity. With the slow synaptic time constant, for example for NMDA receptor, the spike-based model could be reduced into a rate model by using the method of averaging as we have discussed in the last chapter.

$$\tau \frac{ds}{dt} + s = \alpha \nu(g_{syn}) \tag{3.4}$$

Since we only consider the period for the persistent activity, the synaptic conductance g_{syn} can be expressed as the sum of the feedback and tonic input $g_{syn} = W_0 s_0 + Ws$. The fixed point of Eq. (3.4) is

$$s = \alpha \nu(g_{syn}) \tag{3.5}$$

When the synaptic conductance g_{syn} is high, function $\nu(\cdot)$ could be approximated

by a linear function $\nu(x) = F_1 x + F_2$ from the analytical discussion in the last chapter. Fig. (3-2) show the linear fit of the function $\nu(g_{syn})$.

After taking the linear approximation of the activation function $\nu(g_{syn})$, the fix point equation could be rewritten as:

$$s = \alpha F_1 W s + \alpha F_1 (W_0 s_0 + F_2) \tag{3.6}$$

Recurrent feedback weight W and tonic neuron synaptic weight W_0 are tuned as the following.

$$W = \frac{1}{\alpha F_1} \tag{3.7}$$

$$W_0 = -\frac{F_2}{aS_0} \tag{3.8}$$

With the tuned synaptic weights, under linear approximation any s could be a solution of the fix point Eq. (3.6). All the fixed points will thus form a continuous line attractor. However, the line attractor only holds when the function $\nu(\cdot)$ is exactly linear. With the original nonlinear model, the system could have only finite number of fixed points. However, with the tuned parameters W and W_0 if the linearization is good enough around certain range of the s, inside this range we would expect that during the gaze-holding period the drift velocity of s, i.e. ds/dt, would be relatively small.

Fig. (3-3) shows the results of a tuned autapse model using the method we have just introduced. The top four panels show the spike trains of the tonic neuron, burst excitatory neuron and burst inhibitory neuron in panel A, B, C, and D respectively. The bottom two panels show the firing rate and channel variable s of the memory neuron during this 6 seconds period. As we can see from either the spike trains or the firing rate of the memory neuron, with the tuned synaptic weights the neural activity of the memory neuron is sustained very well during every 1 second gaze-holding period.

3.2 Recurrent network model

In the autapse model, we only considered the localized positive feedback. In this section, a distributed feedback model will be considered and we will show how to tune these distributed synaptic weights to produce the persistent neural activities.

As being introduced in the last chapter, the spike-based network model could be reduced to the rate-based recurrent network model described by the dynamics of the channel variable s_i by using the method of averaging.

$$\tau \dot{s}_i + s_i = \alpha f(g_i^{syn}) \tag{3.9}$$

$$g_i^{syn} = \sum_j W_{ij} s_j + b_i \tag{3.10}$$

where b_i is from the tonic neuron input $b_i = W_{0,i} s_{o,i}$.

We have mentioned that the firing rate of the memory neurons holds a linear relationship to the eye position. This means that there is only one degree of freedom in the activities of memories neurons and is parametrized by the eye position. However, in the recurrent network the activities of neurons is normally determined by N modes where N is the total number of neurons. In the linear network, the neuron activity is one point in the state space spanned by the eigenvectors of the weight matrix W with the relative weight determined by the corresponding eigenvalues. In the positive network model we are considering, for the neural activity to be determined mostly by one mode, we should tune the weight matrix such that only one mode will dominate.

In the Wilson-Cowan form network Eq. (3.9), for simplicity we will choose he synaptic matrix W to be of the outer product form.

$$W_{ij} = \xi_i \eta_j \tag{3.11}$$

The meaning of this weight matrix basically states that the every neuron j influence the whole population with the same pattern ξ_i of interaction, only up to some scale factor η_j.

Matrix W with the out product form will make the tuning process much eas-

ier, although it may not be biophysically plausible. It is rank 1 matrix and have only one nonzero eigenvalue. In the following tuning process, only the eigenvector corresponding to the nonzero eigenvalue will be amplified.

With this outer product form of weight matrix W, the synaptic conductance becomes

$$\begin{aligned} g_i^{syn} &= \sum_j W_{ij} + b_i && (3.12) \\ &= \xi_i \sum_j \eta_j s_j + b_i && (3.13) \\ &= \xi_i e + b_i && (3.14) \end{aligned}$$

where we have defined the variable

$$e = \sum_j \eta_j s_j \tag{3.15}$$

The vector $g_i^{syn} = \xi_i e + b_i$ constitutes a line in the N-dimensional space and the variable e determines the position on the line. The variable e is sometimes called the internal representation of the eye position. The motor plant controlling the extraocular muscle is modeled as

$$\tau_E \frac{dE}{dt} + E = c(\sum_j \eta_j s_j + 0.12 s_+ - 0.07 s_-) \tag{3.16}$$

where the variable E is the eye position. During the gaze-holding period, the dynamics becomes

$$\tau_E \frac{dE}{dt} + E = ce \tag{3.17}$$

Thus the eye position E is the low-pass filtering version of the internal representation variable e.

The fixed point equations of Eq. (3.9) are

$$s_i = \alpha f(\sum_j W_{ij} s_j + b_i) \tag{3.18}$$

Substitute this back to the definition of the variable e. We have a close form equation for the variable e to satisfy.

$$e = \alpha \sum_i \eta_i f(\xi_i e + b_i) \tag{3.19}$$

We have discussed in the previous chapter that the activation function $f(\cdot)$ could be approximated well by a linear function. Next we will take this linear approximation and show that under this approximation we could tune the synaptic weight such that any continuous value of e could be end up with the fixed point.

Substituting function f with a linear approximation, we have

$$\begin{aligned} e &= \alpha \sum_i \eta_i [F_1(\xi_i e + b_i) + F_2] && (3.20) \\ &= (\alpha F_1 \sum_i \eta_i \xi_i) e + \alpha \sum_i \eta_i (F_1 b_i + F_2) && (3.21) \end{aligned}$$

The synaptic weights are tuned such that the following equations are satisfied.

$$\begin{aligned} \sum_i \eta_i \xi_i &= \frac{1}{\alpha F_1} && (3.22) \\ \sum_i \eta_i (F_1 b_i + F_2) &= 0 && (3.23) \end{aligned}$$

After following the tuning of synaptic weights, any continuous value of e could be the fixed point solution under the linear approximation. In the original network model, under the tuning we will expect that the drift of memory neuron activities would be relatively small when the synaptic conductances are in the range when the linear approximation is good.

Another way to estimate the tuning parameters is to solve the following least

square error optimization problem

$$\min \int_{e_0}^{e_1} (e - \alpha \sum_i \eta_i f(\xi_i e + b_i))^2 de \tag{3.24}$$

with the range $[e_0, e_1]$ chosen in the biophysically feasible region. This way, we tune the weight matrix W directly without resorting to the linear approximation. This second method is much better when we consider the saturation influence in the dynamical equation of the channel variables, in which case the activation function will appear to be highly nonlinear.

Fig. (3-4) shows that tuned result of the synaptic weight variable ξ and η for a network of 50 memory neurons. In the tuning, the vector ξ is taken to be constant 1, the tonic input vector b is uniformly taken from 0 to 0.0087, and the vector η is taken to be the optimal value that minimize Eq. (3.24). Vector η and b are listed in Table (3.2). The optimal value of η are also plotted in the top right panel of Fig. (3-4). In the bottom two panels of Fig. (3-4) we show how good the tuning is. Shown in the bottom left panel is the relationship between function $f(\xi_i e + b_i)$ and the variable e weighted by parameter η_i for every neuron in the network. As we have discussed before, the function $f(\xi_i e + b_i)$ is the equilibrium value of the dynamical channel variable s_i. Thus this panel basically plots the contribution of every neuron to the motor neuron plant as a function of the internal eye position variable e. The summation of the contributions from all neurons in the network is plot in the bottom right panel, which approximate very well the value e.

After tuning all the synaptic weights, we simulate this 50-neuron network. The result of the simulation is shown in Fig. (3-5). Plot in the top panel is the spike trains of these 50 neurons during a period of 10 seconds with 10 different eye positions. Shown in the middle panel is the firing rate of 10 neurons indicated with different colors. The bottom panel plots the variable e, which is the internal representation of the eye position. As we can see from either spikes trains or the firing rates, with the tuned synaptic weights the memory neurons can fairly well maintain a persistent neural activities at each gaze-holding period.

$1000*\eta$	$100*b$	$1000*\eta$	$100*b$
0.38100	0.87000	0.27582	0.42714
0.99952	0.85228	0.27247	0.409428
0.78117	0.83457	0.27796	0.391714
0.66314	0.81685	0.26595	0.374000
0.58845	0.79914	0.26383	0.356285
0.55034	0.78142	0.26200	0.338571
0.49099	0.76371	0.25956	0.320857
0.46018	0.74600	0.26510	0.303142
0.43476	0.72828	0.25399	0.285428
0.41312	0.71057	0.25309	0.267714
0.40483	0.69285	0.25120	0.250000
0.37488	0.67514	0.25737	0.232285
0.36346	0.65742	0.24721	0.214571
0.35135	0.63971	0.24621	0.196857
0.35114	0.62200	0.24534	0.179142
0.32996	0.60428	0.24390	0.161428
0.32274	0.58657	0.24972	0.143714
0.31594	0.56885	0.23987	0.126000
0.31082	0.55114	0.23977	0.108285
0.31076	0.53342	0.23855	0.090571
0.29503	0.51571	0.24493	0.072857
0.29243	0.49800	0.23580	0.055142
0.28770	0.48028	0.23545	0.037428
0.29213	0.46257	0.23778	0.019714
0.27837	0.44485	0.20415	0.002000

Table 3.1: Tuned η and b_0 for 50 neurons. Listed in the left table is for first 25 neurons and right for the other 25 neurons.

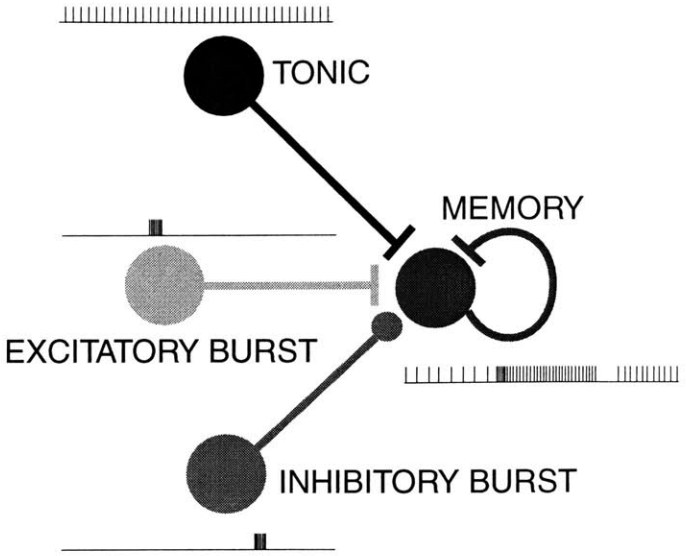

Figure 3-1: Circuit diagram for autapse model

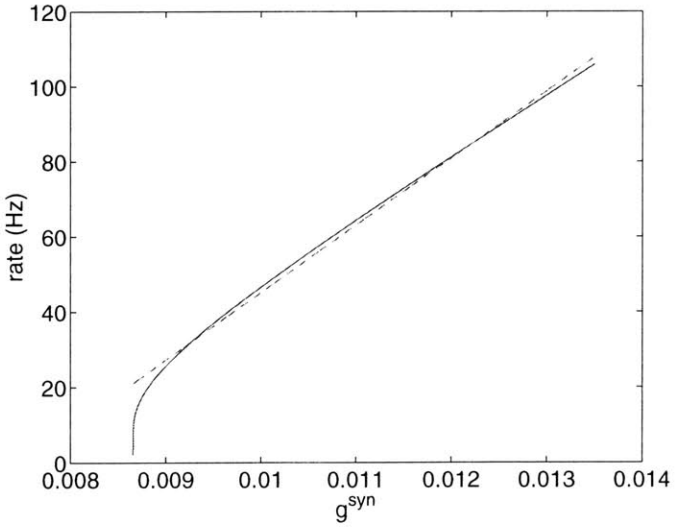

Figure 3-2: Linear approximation of function $\nu(g_{syn})$. In the autapse model we introduced in this chapter, function $\nu(g_{syn})$ is the firing rate of the memory neuron. The domain for the linear approximation is chosen in a physiologically feasible region for the firing rate to be between 20 and 120 Hz.

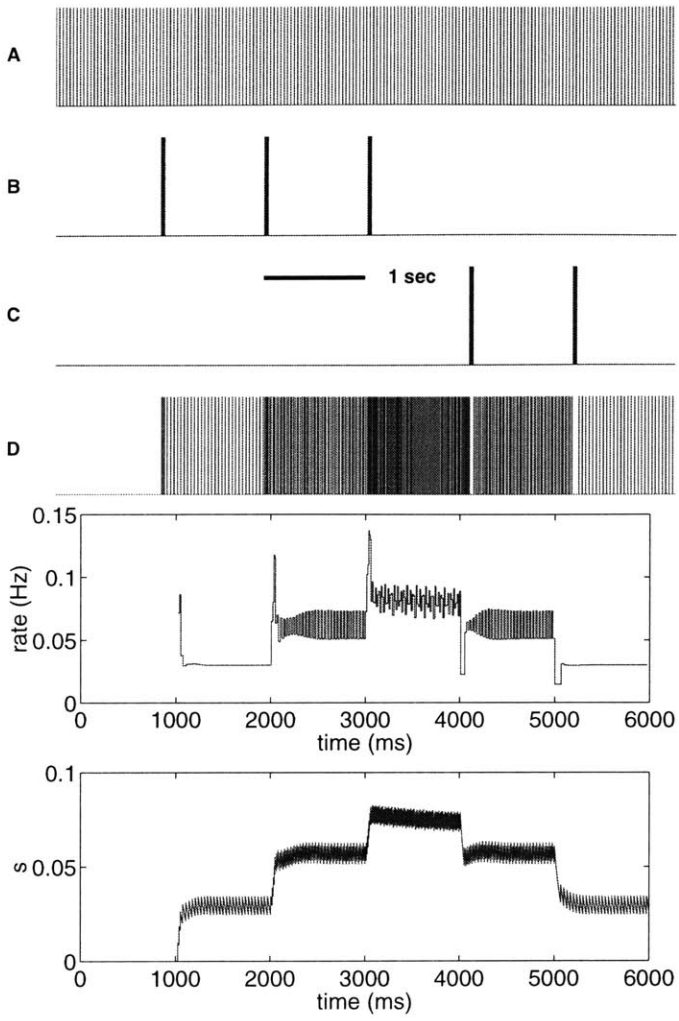

Figure 3-3: The autapse with tuned synaptic weight. The top four panels show the spike trains of the tonic neuron, burst excitatory neuron, burst inhibitory neuron and memory neuron in panel A, B, C, D respectively during a period of 6 seconds. The bottom two panels show the firing rate and the channel variable s of the memory neuron. As we can see from this figure, with the tuned synaptic weights the memory neuron is able to maintain a persistent activity after each saccade. The synaptic weights are tuned in the following values: $W_0 = 0.257$, $W = 0.0596$.

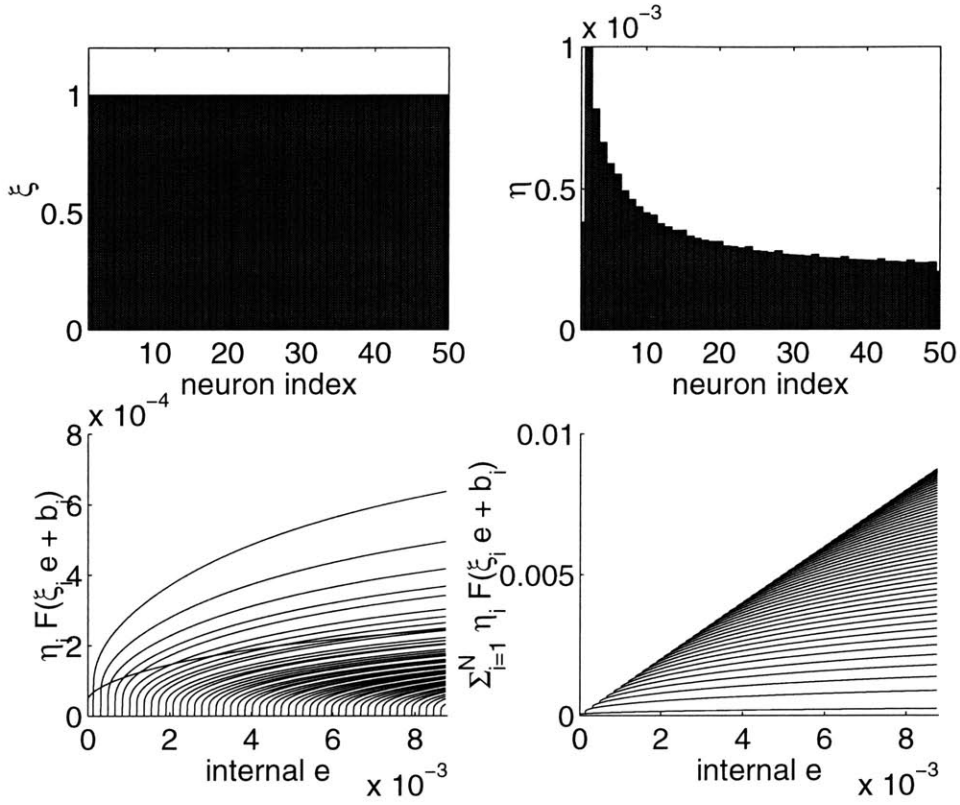

Figure 3-4: Tuned synaptic weight for a recurrent network of 50 memory neurons. The tuned values for vector ξ and η are plotted in the top two panels. Shown in the bottom left panel is the relationship between function $f(\xi_i e + b_i)$ and the variable e weighted by parameter η_i for every neuron in the network. The summation of these weighted functions is show in the bottom right panel gradually with the increased number of neurons.

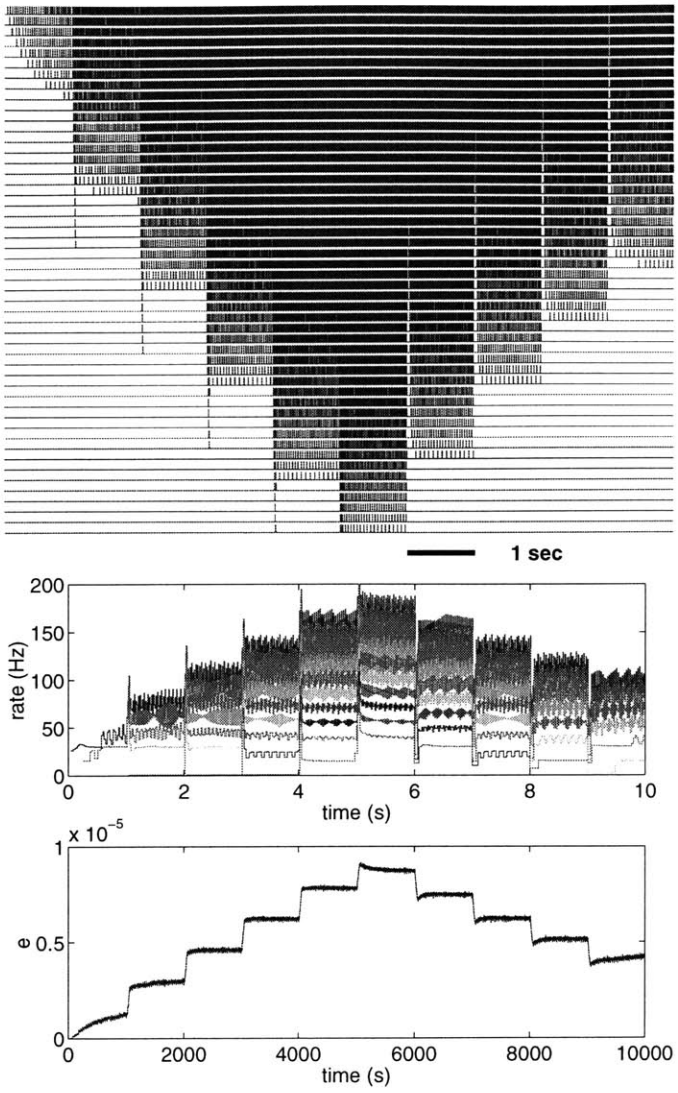

Figure 3-5: Simulation of the recurrent network with 50 memory neurons. Plot in the top panel is the spike trains of these 50 neurons during a period of 10 seconds with 10 different eye positions. Shown in the middle panel is the firing rate of 10 neurons indicated with different colors. The bottom panel plots the variable e, which is the internal representation of the eye position. As we can see from either spikes trains or the firing rates, with the tuned synaptic weights the memory neurons can fairly well maintain a persistent neural activities at each gaze-holding period.

Chapter 4

Learning the stabilization of persistent neural activity

4.1 Introduction

Recent experiments have demonstrated types of synaptic plasticity that depend on the temporal ordering of presynaptic and postsynaptic spiking. At cortical[25] and hippocampal[26] synapses, long-term potentiation is induced by repeated pairing of a presynaptic spike and a succeeding postsynaptic spike, while long-term depression results when the order is reversed. The dependence of the change in synaptic strength on the difference $\Delta t = t_{post} - t_{pre}$ between postsynaptic and presynaptic spike times has been measured quantitatively. This *pairing function*, sketched in Fig. (4-1)A, has positive and negative lobes correspond to potentiation and depression, and a width of tens of milliseconds. We will refer to synaptic plasticity associated with this pairing function as differential Hebbian plasticity—*Hebbian* because the conditions for potentiation are as predicted by Hebb[23], and *differential* because it is driven by the difference between the opposing processes of potentiation and depression.

The pairing function of Fig. (4-1 A) is not characteristic of all synapses. For example, an opposite temporal dependence has been observed at electrosensory lobe synapses of electric fish[24]. As shown in Fig. (4-1 B), these synapses depress when a presynaptic spike is followed by a postsynaptic one, and potentiate when the order

is reversed. We will refer to this as differential anti-Hebbian plasticity.

According to these experiments, the maximum ranges of the Hebbian and anti-Hebbian pairing functions are roughly 20 and 40 ms, respectively. This is fairly short, and seems more compatible with descriptions of neural activity based on spike timing rather than instantaneous firing rates[31, 32]. In fact, we will show that there are two limits in which spike-based learning rules can be approximated by rate-based learning rules. If the pairing range is long, then rate-based learning can be a good approximation on short time scales. If the pairing range is short, then the rate-based approximation can be valid when averaged over long times. Such averaging is relevant when synapses are assumed to learn slowly. In both limits, the rate-based approximation also requires that spike synchrony be small, or have little effect due to the shape of the pairing function.

The pairing functions of Fig. (4-1)A and B lead to rate-based learning rules like those traditionally used in neural networks, except that they depend on temporal derivatives of firing rates as well as firing rates themselves. We will argue that the differential anti-Hebbian learning rule of Fig. (4-1B) could be a general mechanism for tuning the strength of positive feedback in networks that maintain a short-term memory of an analog variable in persistent neural activity[33]. A number of recurrent network models have been proposed to explain memory-related neural activity in motor [34] and prefrontal[35] cortical areas, as well as the head direction system [4] and oculomotor integrator[3, 36, 1]. All of these models require precise tuning of synaptic strengths in order to maintain continuously variable levels of persistent activity. We demonstrate that such tuning can be performed by differential anti-Hebbian learning in a simple model of persistent activity maintained by an integrate-and-fire neuron with an excitatory autapse.

4.2 Spike-based learning rule

Pairing functions like those of Fig. (4-1) have been measured using repeated pairing of a single presynaptic spike with a single postsynaptic spike. Quantitative measure-

ments of synaptic changes due to more complex patterns of spiking activity have not yet been done. We will assume a simple model in which the synaptic change due to arbitrary spike trains is the sum of contributions from all possible pairings of presynaptic with postsynaptic spikes. The model is unlikely to be an exact description of real synapses, but could turn out to be approximately valid.

We will write the spike train of the ith neuron as a series of Dirac delta functions, $s_i(t) = \sum_n \delta(t - T_i^n)$, where T_i^n is the nth spike time of the ith neuron. The synaptic weight from neuron j to i at time t is denoted by $W_{ij}(t)$. Then the change in synaptic weight induced by presynaptic spikes occurring in the time interval $[0, T]$ is modeled as

$$W_{ij}(T + \tau) - W_{ij}(\tau) = \int_0^T dt_j \int_{-\infty}^{\infty} dt_i \, f(t_i - t_j) s_i(t_i) \, s_j(t_j) \tag{4.1}$$

Each presynaptic spike is paired with all postsynaptic spikes produced before and after. Because each presynaptic spike results in induction of plasticity only after a time delay of τ, the arguments $T+\tau$ and τ of W_{ij} on the left hand side of the equation are shifted relative to the limits T and 0 of the integral on the right hand side. The length τ of the shift is assumed to be greater than the width of the pairing function f, so that $f(\tau) \approx 0$. With this assumption, W_{ij} at time $T + \tau$ is only influenced by spikes that happened before that time, and therefore the learning rule is causal.

There is some subtlety involved in our choice of the limits of integration in Eq. (4.1). These limits will be important for the numerical simulations to be discussed later, in which there is an external control signal that gates plasticity on and off. Then Eq. (4.1) is the change that results when the control signal activates plasticity from time 0 to T. Another possible definition would have been to place the $[0, T]$ limits on the integral over the postsynaptic spike, rather than the presynaptic spike. This alternative leads to some differences in learning behavior, but can still be analyzed using the methods of this paper.

4.3 Relation to rate-based learning rules

The learning rule of Eq. (4.1) is driven by correlations between presynaptic and postsynaptic activities. This dependence can be made explicit by making the change of variables $u = t_i - t_j$ in Eq. (4.1), which yields

$$W_{ij}(T+\tau) - W_{ij}(\tau) = \int_{-\infty}^{\infty} du f(u) C_{ij}(u) \tag{4.2}$$

where we have defined the cross-correlation

$$C_{ij}(u) = \int_0^T dt\, s_i(t+u)\, s_j(t)\ . \tag{4.3}$$

Often it is also possible to define a cross-correlation between firing rates,

$$C_{ij}^{rate}(u) = \int_0^T dt\, \nu_i(t+u)\, \nu_j(t) \tag{4.4}$$

For example, this can be calculated during repeated presentations of a stimulus by techniques such as the shift predictor. In other situations, it may be possible to define instantaneous firing rates in some other manner, such as temporal filtering of the spike train. The "rate correlation" is commonly subtracted from the total correlation to obtain the "spike correlation" $C_{ij}^{spike} = C_{ij} - C_{ij}^{rate}$.

To derive a rate-based approximation to the learning rule (4.2), we rewrite it as

$$W_{ij}(T+\tau) - W_{ij}(\tau) = \int_{-\infty}^{\infty} du\, f(u) C_{ij}^{rate}(u) + \int_{-\infty}^{\infty} du\, f(u) C_{ij}^{spike}(u) \tag{4.5}$$

and simply neglect the second term. Shortly we will discuss the conditions under which this is a good approximation. But first we derive another form for the first term,

$$\int_{-\infty}^{\infty} du f(u) C_{ij}^{rate}(u) \approx \int_0^T dt[\beta_0 \nu_i(t) + \beta_1 \dot{\nu}_i(t)] \nu_j(t) \tag{4.6}$$

by defining

$$\beta_0 = \int_{-\infty}^{\infty} du f(u) \qquad \beta_1 = \int_{-\infty}^{\infty} du\, u f(u) \tag{4.7}$$

and applying the approximation $\nu_i(t+u) \approx \nu_i(t) + u\dot{\nu}_i(t)$, which makes sense when firing rates vary slowly on the time scale of the pairing function. This result means that the learning rule is dependent not only on firing rates but also on their time derivatives.

The pairing functions shown in Fig. (4-1)A and B have both positive and negative lobes. If the areas under both lobes exactly cancel, then $\beta_0 = 0$, so that the dependence on postsynaptic activity is purely on the time derivative of the firing rate. Hebbian learning corresponds to $\beta_1 > 0$ (Fig. (4-1 A), while anti-Hebbian learning leads to $\beta_1 < 0$ (Fig. (4-1 B)). To summarize, the synaptic changes due to rate correlations are given by

$$\dot{W}_{ij} \propto \dot{\nu}_i \nu_j \quad \text{(Hebbian)} \qquad \dot{W}_{ij} \propto -\dot{\nu}_i \nu_j \quad \text{(anti-Hebbian)} \tag{4.8}$$

for slowly varying rates. These formulas imply that a constant postsynaptic firing rate causes no net change in synaptic strength. Instead, changes in rate are required to induce synaptic plasticity.

To illustrate this point, Fig. (4-1C) shows the result of applying differential anti-Hebbian learning to two Poisson spike trains. The rate of the presynaptic spike train is constant at 50 Hz, while that of the postsynaptic spike train shifts from 50 Hz to 200 Hz at 1000 ms. While the firing rates are constant, the synaptic strength fluctuates but remains roughly constant. But the upward shift in firing rate causes a downward shift in synaptic strength, in accord with the sign of the anti-Hebbian rule in Eq. (4.8).

The rate-based approximation works well for this example, because the second term of Eq. (4.5) is not so important. Let us return to the issue of the general conditions under which this term can be neglected. With Poisson spike trains, the spike correlations are zero on average, so that the second term of Eq. (4.5) fluctuates

about zero. There are two conditions under which these fluctuations are small: a large pairing range or a long time period T of learning. In Fig. (4-1)C we have used a relatively long pairing range of 100 ms, so that the fluctuations are small even over short periods of learning. If a short pairing range were used, the fluctuations would still go to zero as the time period T of learning increased. This sort of averaging is relevant if the rate of learning is very slow.

In the brain, nonvanishing spike correlations are sometimes observed even after averaging. In the common case where these correlations are symmetric about zero, then they will produce little plasticity if the pairing functions are antisymmetric as in Fig. (4-1)A and B. On the other hand, if the spike correlations are asymmetric, they could lead to substantial effects[32].

4.4 Effects on recurrent network dynamics

The learning rules of Eq. (4.8) depend on both presynaptic and postsynaptic rates, like learning rules conventionally used in neural networks. They have the special feature that they depend on time derivatives, which has computational consequences for recurrent neural networks of the form

$$\tau \dot{x_i} + x_i = \sum_j W_{ij}\sigma(x_j) + b_i \tag{4.9}$$

Such classical neural network equations can be derived from more biophysically realistic models using the method of averaging[37] or a mean field approximation[38]. The firing rate of neuron j is conventionally identified with $\nu_j = \sigma(x_j)$.

The cost function

$$E(\{x_i\};\{W_{ij}\}) = \frac{1}{2}\sum_i \dot{\nu}_i^2 \tag{4.10}$$

quantifies the amount of drift in firing rate at the point $x_1, \ldots, x_N$ in the state space of the network. If we consider $\dot{\nu}_i$ to be a function of x_i and W_{ij} defined by (4.9),

then the gradient of the cost function with respect to W_{ij} is given by

$$\partial E/\partial W_{ij} = \sigma'(x_i)\dot{\nu}_i\nu_j. \tag{4.11}$$

Assuming that σ is a monotonically increasing function so that $\sigma'(x_i) > 0$, it follows that the Hebbian update of (4.8) increases the cost function, and hence increases the magnitude of the drift velocity. In contrast, the anti-Hebbian update decreases the drift velocity. This suggests that the anti-Hebbian update could be useful for creating fixed points of the network dynamics (4.9).

4.5 Persistent activity in a spiking autapse model

The preceding arguments about drift velocity were based on approximate rate-based descriptions of learning and network dynamics. It is important to implement spike-based learning in a spiking network dynamics, to check that our approximations are valid.

Therefore we have numerically simulated the simple recurrent neural circuit of integrate-and-fire neurons shown in Fig. (3-1). The core of the circuit is the "memory neuron," which makes an excitatory autapse onto itself. It also receives synaptic input from three input neurons: a tonic neuron, an excitatory burst neuron, and an inhibitory burst neuron. It is known that this circuit can store a short-term memory of an analog variable in persistent activity, if the strength of the autapse and tonic synapse are precisely tuned[1]. Here we show that this tuning can be accomplished by the spike-based learning rule of Eq. (4.1), with a differential anti-Hebbian pairing function like that of Fig. (4-1 B).

The memory neuron is described by the equations

$$C_m\frac{dV}{dt} = -g_L(V - V_L) - g_E(V - V_E) - g_I(V - V_I) \tag{4.12}$$

$$\tau\frac{ds}{dt} + s = \alpha_s\sum_n \delta(t - T_n) \tag{4.13}$$

where V is the membrane potential, $C_m = 1$ nF is the membrane capacitance, $g_L = 0.025$ μS is the leak conductance, and $V_L = -70$ mV is the leak potential. There are excitatory and inhibitory synaptic conductances g_E and g_I, with reversal potentials of $V_E = 0$ mV, and $V_I = -70$ mV. When V reaches the threshold -52 mV, an action potential is considered to have occurred, and V is reset to -59 mV. Each spike at time T_n causes a jump in the synaptic activation s of size α_s/τ, where $\alpha_s = 1$, after which s decays exponentially with time constant $\tau = 100$ ms until the next spike.

The synaptic conductances of the memory neuron are given by

$$g_E = Ws + W_0 s_0 + W_+ s_+ \qquad g_I = W_- s_- \tag{4.14}$$

The term Ws is recurrent excitation from the autapse, where W is the strength of the autapse. The synaptic activations s_0, s_+, and s_- of the tonic, excitatory burst, and inhibitory burst neurons are governed by equations like (4.12) and (4.13), with a few differences. Each of these neurons has no synaptic input; its firing pattern is instead determined by an applied current. The tonic neuron has an applied current of 0.5203 nA, which makes it fire repetitively at roughly 20 Hz. Its synaptic time constant is $\tau_0 = 100$ ms. For the excitatory and inhibitory burst neurons the applied current is normally zero, except for brief 100 ms current pulses of 0.95 nA that cause bursts of action potentials. Their synaptic time constants are $\tau_+ = \tau_- = 5$ ms. The excitatory and inhibitory burst synapses have strengths $W_+ = 0.1$ and $W_- = 0.05$.

As shown in Fig. (4-2), if the synaptic strengths W and W_0 are not tuned, the burst neurons cause only transient changes in the firing rate of the memory neuron. After applying the spike-based learning rule (4.1) to tune both W and W_0, the memory neuron is able to maintain persistent activity. During the interburst intervals (from τ after one burst until τ before the next), we made synaptic changes using the anti-Hebbian pairing function $f(t) = -A\sin(\pi t/\tau)$ for spike time differences in the range $[-\tau, \tau]$ with $A = 1.5 \times 10^{-4}$ and τ=120 ms. The resulting increase in persistence time can be seen in Fig. (4-3 A), along with the values of the synaptic weights versus time.

To quantify the performance of the system at maintaining persistent activity, we

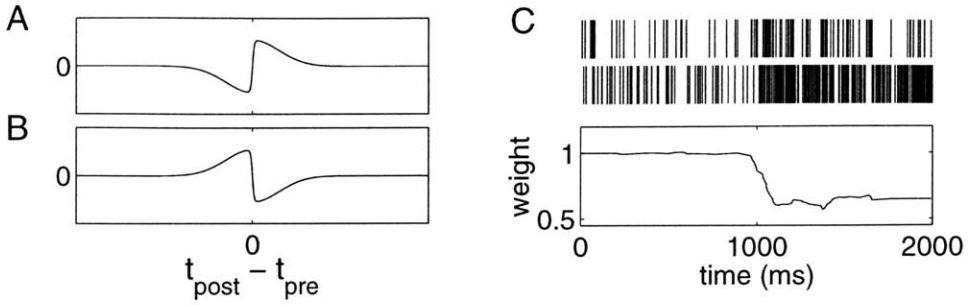

Figure 4-1: (A) Pairing function for differential Hebbian learning. The change in synaptic strength is plotted versus the time difference between postsynaptic and presynaptic spikes. (B) Pairing function for differential anti-Hebbian learning. (C) Differential anti-Hebbian learning is driven by changes in firing rates.

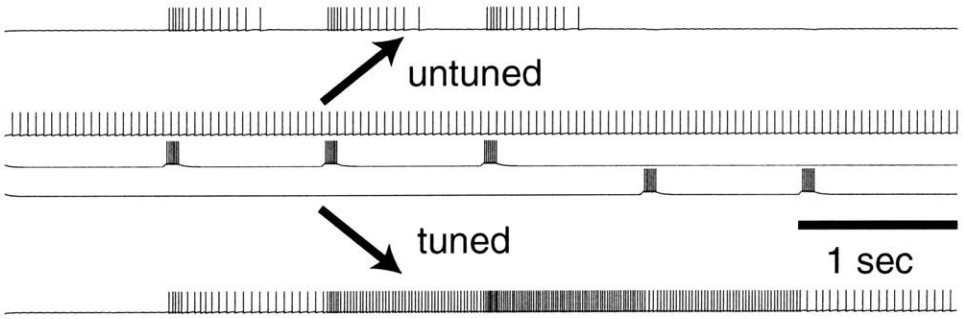

Figure 4-2: Untuned and tuned autapse activity. The middle three traces are the membrane potentials of the three input neurons in Fig. (4-2) 2 (spikes are drawn at the reset times of the integrate-and-fire neurons). If the strengths W and W_0 of the autapse and tonic synapse are not tuned, then the activity of the memory neuron is not persistent, as shown in the top trace. Once these parameters are tuned, then the burst inputs cause persistent changes in activity.

determined the relationship between $d\nu/dt$ and ν using a long sequence of interburst intervals. If W and W_0 are fixed at optimally tuned values, there is still a residual drift, as shown in Fig. (4-3) [1]. But if these parameters are allowed to adapt continuously, even after good tuning has been achieved, then the residual drift is even smaller in magnitude. This is because the learning rule tweaks the synaptic weights during each interburst interval, reducing the drift for that particular firing rate.

Autapse learning is driven by the autocorrelation of the spike train, rather than a cross-correlation. The peak in the autocorrelogram at zero lag has no effect, since the pairing function is zero at the origin. Since the autocorrelation is zero for small time lags, we used a fairly large pairing range in our simulations. In a recurrent network of many neurons, a shorter pairing range would suffice, as the cross-correlation does not vanish near zero.

4.6 Discussion

We have shown that differential anti-Hebbian learning can tune a recurrent circuit to maintain persistent neural activity. This behavior can be understood by reducing the spike-based learning rule (4.1) to the rate-based learning rules of Eqs. (4.6) and (4.8). The rate-based approximations are good if two conditions are satisfied. First, either the width of the pairing function must be large, or the rate of learning must be slow. Second, spike synchrony must be weak, or have little effect on learning due to the shape of the pairing function.

The differential anti-Hebbian pairing function results in a learning rule that uses $-\dot{\nu}_i$ as a negative feedback signal to reduce the amount of drift in firing rate, as illustrated by our simulations of an integrate-and-fire neuron with an excitatory autapse. More generally, the learning rule could be relevant for tuning the strength of positive feedback in networks that maintain a short-term memory of an analog variable in persistent neural activity[33]. For example, the learning rule could be used to improve the robustness of the oculomotor integrator[3, 36, 1] and head direction system[4] to mistuning of parameters. In deriving the differential forms of the learning rules in

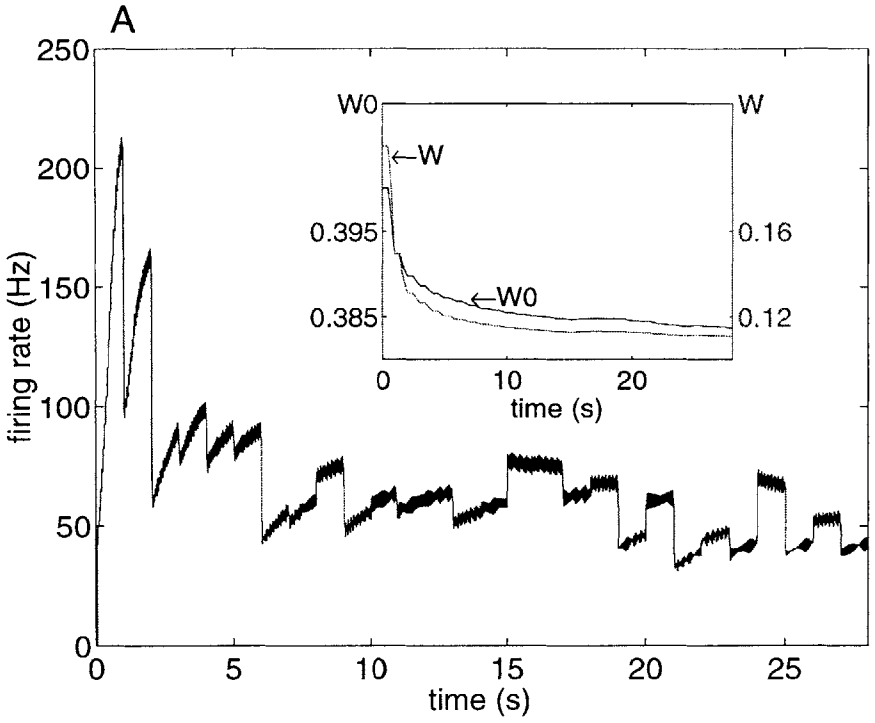

Figure 4-3: Tuning the autapse. The persistence time of activity increases as the weights W and W_0 are tuned. Each transition is driven by pseudo-random bursts of input. The update of both tonic and recurrent synaptic weights is also shown.

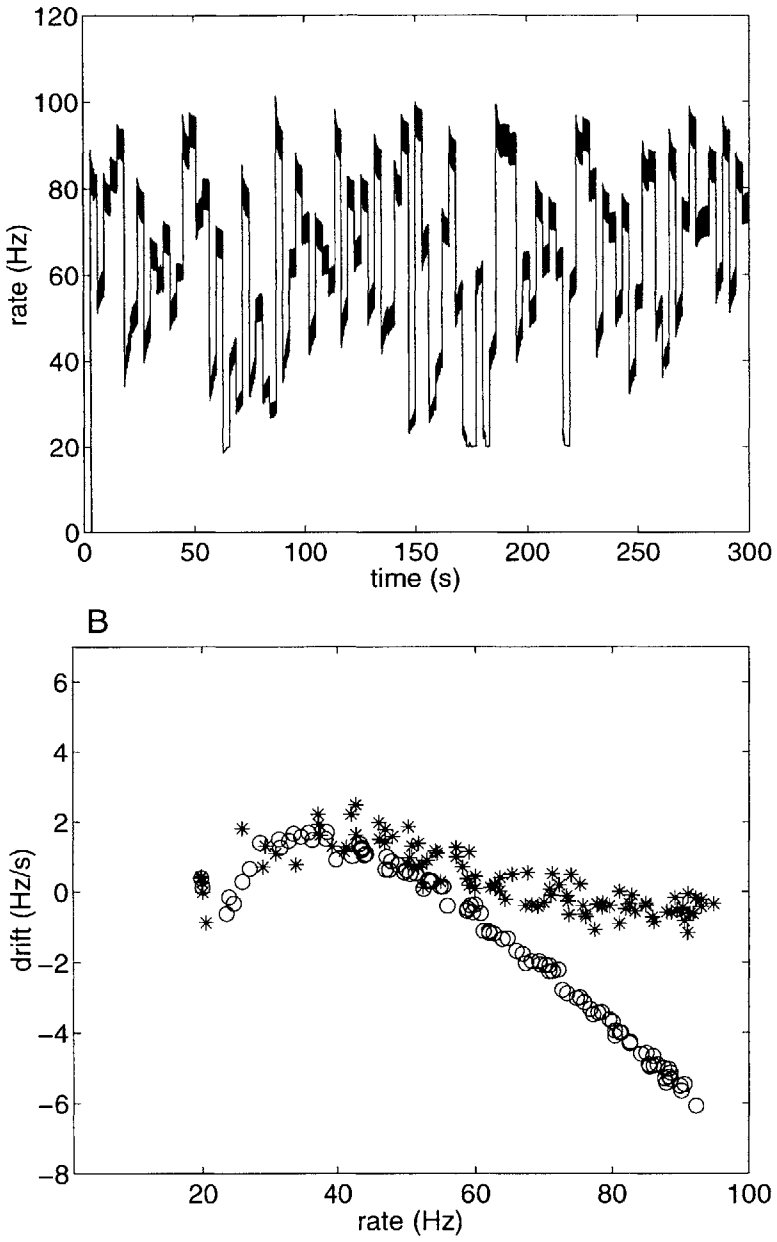

Figure 4-4: Shown in the top panel is the firing rate of the memory neuron during 300 seconds following the sequence of random saccades. In bottom panel, shown is the systematic relationship between drift $d\nu/dt$ in firing rate and ν, as measured from a long sequence of inter-burst intervals. If the weights are continuously fine-tuned ('*') the drift is less than with fixed well-tuned weights ('o').

(4.8), we assumed that the areas under the positive and negative lobes of the pairing function are equal, so that the integral defining β_0 vanishes. In reality, this cancellation might not be exact. Then the ratio of β_1 and β_0 would limit the persistence time that can be achieved by the learning rule.

Both the oculomotor integrator and the head direction system are also able to integrate vestibular inputs to produce changes in activity patterns. The problem of finding generalizations of the present learning rules that train networks to integrate is still open[33].

Chapter 5

Learning VOR

5.1 Introduction

The vestibular-occular-refex(VOR) is an important function for the neural system to keep a still visual image for processing while the head is moving. The neural system accomplishes this by correspondingly moving the eye to compensate the positional change of the moving object such that the object could still project to the same position on the retina.

The VOR involves the close coordination between the vestibular and oculomotor systems. When the head is moving, the peripheral vestibular system inside the inner ear detects its motion and sends the afferent to the vestibular neurons in the brain stem. It has been observed that the firing rate of the vestibular neuron is an affine function of the head velocity. When the head velocity is zero, there is a tonic background activity in the vestibular neuron with a firing rate ranging from 10-60Hz (We referred the neuron with tonic activity as the tonic neuron in previous chapters). When the head is moving, the changed firing rate in the vestibular neuron would be linearly correlated to the head velocity $\dot{H}$. The firing rate of vestibular neuron can be expressed as

$$b = \beta \dot{H} + b_0 \tag{5.1}$$

where b_0 is the background activity when the head velocity is zero. We will define the variable $\delta b_i = b_i - b_{0,i}$ which will code the head position information for neuron i.

The vestibular neuron sends its input to the integrator neuron, where the head velocity signal will be integrated into position signal in the integrator. The firing rate of the integrator neuron will thus code the information about desired eye position being used to compensate the head movement.

5.2 Learning

In the reduced model after using the method of averaging, the activity of the integrator neuron is described by the channel variable s_i.

$$\begin{aligned} \tau_i \dot{s}_i + s_i &= f(g_i) && (5.2) \\ &= f(\sum_{j=1}^{N} W_{ij} s_j + b_i) && (5.3) \end{aligned}$$

were $b_i = w_{0,i} s_{0,i}$ is the input from the vestibular neuron.

However, the channel variable s_i is not a good candidate to describe the activity of a neuron, which is normally characterized by its firing rate. The synaptic conductance g_i describe the firing rate of the neuron more closely than channel variable s_i. The firing rate of neuron i is determined by the function of g_i expressed as $\nu_i = f(g_i)$. Since the function $f(g_i)$ can be reasonably well approximated by a linear function, the variable g_i is directly related to the firing rate. In the following, we will describe the dynamics of neuron i by using the variable g_i rather than s_i.

If the time constant $\tau_i = \tau_j$ for all j, the dynamical Eq. (5.2) can be converted into the dynamics of variable g_i by taking derivative on both side of the following equation and substitute $\dot{s}_i$ with Eq. (5.2).

$$g_i = \sum_j w_{ij} s_j + b_i \qquad (5.4)$$

The resulted dynamics of g_i is described by the following equation.

$$\tau \dot{g}_i + g_i = \sum_{i=1}^{N} W_{ij} f(g_j) + b_i \tag{5.5}$$

To learn to hold persistent activity during gaze-holding period, we formulate the following error function to be minimized at each gaze-holding period.

$$E = \frac{1}{2} \sum_{i=1}^{N} \dot{g_i}^2 \tag{5.6}$$

The error function E will be large if the drift velocity of the memory neuron firing rate is high and the minimum of E is reached if and only if the drift velocity of every neuron is zero.

We view the learning as an optimization problem by minimizing the error function E through constantly updating the synaptic weights. Let's take the gradient decent method.

$$\Delta W_{ij} \sim -\frac{\partial E}{\partial W_{ij}} \tag{5.7}$$

$$= -\frac{1}{\tau} \dot{g}_i f(g_i) \tag{5.8}$$

$$= -\frac{1}{\tau f'(g_i)} \dot{\nu}_i \nu_j \tag{5.9}$$

Since function $f(\cdot)$ is roughly a linear function, the derivative could be approximated by a constant. So the update rule for the weight W_{ij} ends up with

$$\Delta W_{ij} \sim -\dot{\nu}_i \nu_j \tag{5.10}$$

This is the differential anti-Hebbian learning rule expressed in the form of firing rates. In the autapse model we have discussed in last chapter, we use this rule to tune the recurrent and tonic weight to stabilize the persistent neural activity during gaze-holding period.

To learn VOR, we can still follow the above similar idea to derive the learning

rule. However a different error function has to be formulated. The error function for learning VOR has to reflect the difference between the velocity difference between the moving head and eye. We will use the following least square error function.

$$E = \frac{1}{2}\sum_{i=1}^{N}(\dot{g}_i - \beta_i \delta b_i)^2 \tag{5.11}$$

In this error function, $\dot{g}_i$ code the information of eye velocity and δb_i code the information of head velocity. β_i is the parameter coding the ratio between eye position and the changed vestibular neuron firing rate δb_i. Thus this error function basically states the inconsistence between head and eye velocity signals.

To minimize the VOR error function, we will update weight W_{ij} by using the gradient descend method. The learning rule becomes:

$$\Delta W_{ij} \sim (\beta_i \delta b_i - \dot{g}_i)\nu_j \tag{5.12}$$

The equilibrium state of this learning rule is

$$\dot{g}_i = \beta_i \delta b_i \tag{5.13}$$

The eye position is controlled by the motor plant dynamics during the gaze-holding period.

$$\tau_E \frac{dE}{dt} + E = c\sum_j \eta_j s_j \tag{5.14}$$

Usually, the time constant τ_E is large. The output eye position is just the low-pass filtering of the internal e multiplied with some scale parameter c. Since the τ_E is large, from the plant dynamics, the eye position would be described approximately by

$$E = c\sum_j \eta_j s_j \tag{5.15}$$

$$= c(g_i - b_i)/\xi_i \tag{5.16}$$

The eye velocity thus reads

$$\begin{aligned}
\dot{E} &= c\sum_j \eta_j \dot{s}_j && (5.17)\\
&= c(\dot{g}_i - \dot{b}_i)/\xi_i && (5.18)\\
&= \frac{c\beta_i}{\xi_i}\delta b_i - \frac{c}{\xi_i}\dot{b}_i && (5.19)\\
&= \frac{c\beta_i}{\xi_i W_{0,i}}\dot{H} - \frac{c}{\xi_i W_{0,i}}\ddot{H} && (5.20)
\end{aligned}$$

Thus at the equilibrium of learning, the time derivative of the motor neuron firing rate is the combination of both head velocity and head acceleration signals. In order to precisely compensate the head movement, the eye velocity signal component of the motor neuron firing rate derivative should be the same as the head velocity signal. Thus the parameter β_i has to satisfy the following condition.

$$\beta_i = \frac{\xi_i W_{0,i}}{c} \tag{5.21}$$

A biophysically plausible update rule for parameter β_i to precisely satisfy the above equation is hard to be found, since β_i is not a biophysical parameter. The difficulty also lies in that β_i depends on vestibular neuron synaptic strength $W_{0,i}$ and recurrent synaptic strength W_{ij} through ξ_i, both of which are adaptively updated during the learning process.

In the following section, we will concentrate on the VOR learning problem on the simplified autapse model. We try to solve the above dilemma by adaptively changing another biophysical parameters – integrator neuron leak conductance g_L. We will show how to adaptive update g_L and the simulation results with learning rules implemented will be presented.

5.3 VOR learning in autapse model

The learning rule we have implemented in the autapse model for learning VOR is

$$\Delta W \sim (\beta\delta\nu_0 - \dot{\nu}))\nu \tag{5.22}$$

$$\Delta W_0 \sim (\beta\delta\nu_0 - \dot{\nu}))\nu_0 \tag{5.23}$$

$$\Delta g_L \sim -(\beta\delta\nu_0 - \dot{\nu}))\nu \tag{5.24}$$

where ν_0 is the firing rate of vestibular neuron and $\delta\nu_0$ is the firing rate after subtracting the background firing rate when the head velocity is zero. The update of the recurrent synaptic strength W and vestibular neuron synaptic strength W_0 follows the mixture of the differential anti-Hebbian and the Hebbian learning rules, while leak conductance for the integrator neurons follows the combination of the differential Hebbian and the Hebbian learning rule.

The leak conductance is closely related to the activity of the neuron. The larger the leak conductance, the less the firing rate would be. The update rule for leak conductance utilize the information about the difference $d = \beta\delta\nu_0 - \dot{\nu}$ to change g_L. If d is positive, this means that the time derivative of integrator neuron firing rate is too low and thus g_L is decreased. In contrast, if d is negative, which means that the time derivative of integrator neuron firing rate is too hight. As a result, g_L will be increased.

Fig. (5-1) shows the firing rates of the integrator neuron with the sinusoid vestibular input with not precisely tuned synaptic weights. The applied current to the vestibular neuron is $I_{app} = 0.5 + 0.005sin(2\pi t/T)$ nA with the period $T = 2$ seconds. The background activity of this vestibular neuron is roughly 33 Hz and the firing rate fluctuates between 31 and 35 Hz representing the moving of head back and forth. With the synaptic weights not precisely tuned, the integrator neuron is not able to precisely integrate the vestibular input. In contrary, Fig. (5-1) shows that the activity of the integrator neuron decays to zero indicating the sign of weak feedback or vestibular input strength.

With the same initially untuned synaptic weights, but with VOR learning rules implemented in the autapse model, neuron is able to change the synaptic weights W and W_0 and leak conductance constantly such that the integrator is able to integrate the vestibular input. Fig. (5-2) shows the the results after the learning. The applied current to the vestibular neuron is the same as in Fig. (5-1). However, this time the integrator neuron is able to integrate the vestibular neuron input and the drift is very low.

5.4 Discussion of learning rule on g_L

In chapter 1, we derive that when g_{syn} is large, the firing rate of the neuron $f(g_{syn})$ could be approximated as a linear function of g_{syn}.

$$\nu(g_{syn}) \approx ag_{syn} + b \tag{5.25}$$

$$F_1 = \frac{1}{C_m ln((V_0 - V_{syn})/(V_{th} - V_{syn}))} \tag{5.26}$$

$$F_2 = g_L \frac{1 - (\frac{V_0 - V_L}{V_0 - V_{syn}} - \frac{V_{th} - V_L}{V_{th} - V_{syn}})[ln((V_0 - V_{syn})/(V_{th} - V_{syn}))]^{-1}}{C_m ln((V_0 - V_{syn})/(V_{th} - V_{syn}))} \tag{5.27}$$

For the recurrent feedback weight W and vestibular neuron synaptic weight W_0 to be precisely tuned, their values have to satisfy the following equations:

$$W = \frac{1}{F_1} \tag{5.28}$$

$$W_0 = -\frac{F_2}{F_1 S_0} \tag{5.29}$$

Thus in the precisely tuned autapse, the recurrent weight does not depend on the leak conductance g_L, while the vestibular synaptic weight W_0 is linearly related to g_L.

$$W_0 \sim g_L \tag{5.30}$$

Thus the update of leak conductance g_L will correspondingly result in the linear

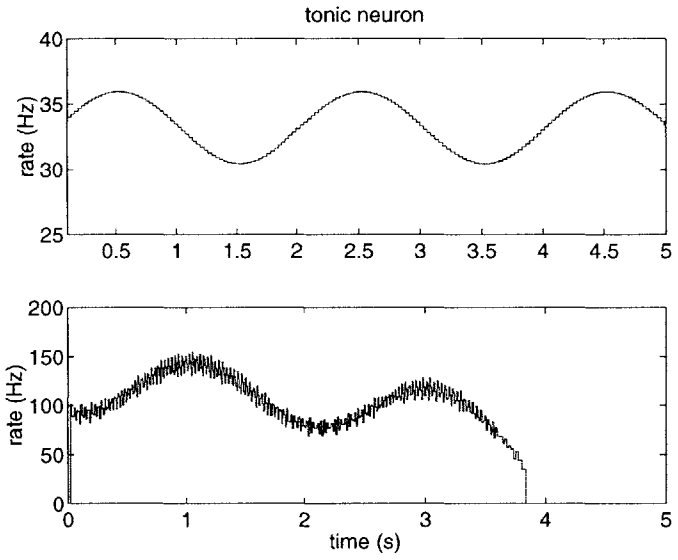

Figure 5-1: Firing rate of the autapse during VOR with untuned weights. The applied current to the vestibular neuron is $I_{app} = 0.5 + 0.005sin(2\pi t/T)$ nA with the period $T = 2$ seconds. Shown in the figure is the firing rate of vestibular and integrator neurons during a period of 5 seconds. The vestibular synaptic weight $W_0 = 0.1978$ recurrent weight $W = 0.0651$ and integrator neuron leak conductance $g_L = 0.025\mu S$. With the untuned weights, the integrator neuron is leaky and the firing rate decays to zero.

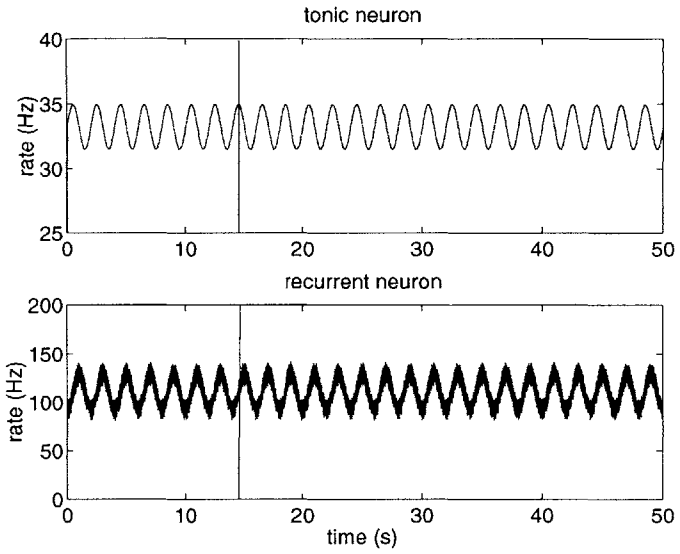

Figure 5-2: Firing rate of the autapse during VOR with learning implemented. The applied current to the vestibular neuron is $I_{app} = 0.5 + 0.005sin(2\pi t/T)$ nA with the period $T = 2$ seconds. Shown in the figure is the firing rate of vestibular and integrator neurons after 100 seconds of learning and still with learning rule implemented during a period of 50 seconds. At the end of the learning, the vestibular synaptic weight $W_0 = 0.2030$, recurrent synaptic weight $W = 0.0642$ and leak conductance $g_L = 0.0249\mu S$. This plot shows that the integrator neuron is able to integrate the vestibular input. The two vertical lines show the anti phase relationship between these two firing rates, which directly results from the integration of a sinusoid function.

change in the target tuned W_0 weight. As we have seen from the constrained Eq. (5.21) for parameter β_i, changing target tuned W_0 weight has to be taken in order to satisfy this equation. The update rule g_L is taken here as an indirect way to satisfy the matching condition between eye and head velocities.

5.5 Discussion

We have shown that the combination of the Hebbian and differential Hebbian learning rules can be used to tune synaptic weights for learning the VOR. The combination of the Hebbian and differential Hebbian learning rules is an extension of the learnings we introduce in the last chapter. It can be derived also from the spike-based learning rules by choosing an asymmetric pairing function.

To learn the right scale relationship between the head and eye velocity, we adaptively update the leak conductance g_L in the integrator neuron. Whether this is biophysically true has to be tested in future experiments.

Chapter 6

Learning in the recurrent network

In the last two chapters, we have discussed two learning cases: a) Learning to hold persistent activity during gaze holding period; b) Learning VOR. Both of these two learning rules are implemented in an autapse model with localized synaptic feedback. Though the autapse model is very simple and is helpful in illustrating several important concepts, whether it is a biophysically plausible model remains arguable. It is critical to check if the learning rules we have discussed could succeed if they are implemented in a recurrent network model.

In the following, we will implement the anti-Hebbian learning rules to stabilizing the persistent neural activity during gaze holding period in the recurrent network model. The network is comprised of three different types of neurons – tonic, burst excitatory, burst inhibitory and memory neurons. Memory neurons receive the input from the tonic and burst neurons, and also the positive feedback from other memory neurons. During every saccade, the burst neuron sends the transient pulse input to the memory neurons, and in a tuned network will lead to the step change in the activities of memory neurons. The goal of the learning is that the memory neurons are able to keep the persistent activity during gaze holding period after each saccade.

We will show the simulation results of two network models, which are the same except the number of memory neurons. In one network, there are only two memory neurons. We choose to study this network because its structure and computation are the simplest among all recurrent networks. The second network is comprised of five

memory neurons.

6.1 Coupled memory neurons

Fig. (6-1) shows a diagram of the coupled two neuron network. In the reduced rate model, the channel variables for memory neuron 1 and 2 can be described by the following two equations.

$$\tau \dot{s_1} + s_1 = f(W_{12}s_2 + b_1) \tag{6.1}$$

$$\tau \dot{s_2} + s_2 = f(W_{21}s_1 + b_2) \tag{6.2}$$

The fixed point equations will be

$$s_1 = f(W_{12}s_2 + b_1) \tag{6.3}$$

$$s_2 = f(W_{21}s_1 + b_2) \tag{6.4}$$

If we take a linear approximation of the function $f(x) = F_1x + F_2$, the fixed point equations becomes

$$s_1 = F_1W_{12}s_2 + F_1b_1 + F_2 \tag{6.5}$$

$$s_2 = F_1W_{21}s_1 + F_1b_2 + F_2 \tag{6.6}$$

Substitute the s_1, s_2 from the other equation, we have

$$s_1 = F_1^2W_{12}W_{21}s_1 + F_1b_1 + F_2 + F_1(F_1b_2 + F_2) \tag{6.7}$$

$$s_2 = F_1^2W_{12}W_{21}s_2 + F_1b_2 + F_2 + F_1(F_1b_1 + F_2) \tag{6.8}$$

If the weights are tuned as the following equation, then the fixed points of s_1 and s_2 becomes a continuous manifold. In phase space, s_1 and s_2 will lie in a line

attractor.

$$W_0 = -\frac{F_2}{F_1 s_0} \tag{6.9}$$

$$W_{12}W_{21} = \frac{1}{F_1^2} \tag{6.10}$$

If synaptic weights are tuned precisely this way, the line attractor in phase space of s_1 and s_2 would be

$$s_1 = \sqrt{\frac{W_{12}}{W_{21}}} s_2 \tag{6.11}$$

Next we will show the simulation result in this positively coupled network model. Two memory neurons receive saccadic input from bust excitatory and burst inhibitory neurons with synaptic strength of 0.08 for both of them. The initial synaptic weights from tonic neurons are $W_0[0] = 0.06292$ and $W_0[1] = 0.06145$. The mutual positive feedback for two memory neurons are $W[0][1] = 0.08295$ and $W[1][0] = 0.08870$. The parameters on all neurons otherwise are the same as those in previous chapters.

The network is run for 100 seconds with learning rules implemented. Every 500 ms, the burst neuron will fire for 50 ms and a random saccade will be initiated.

Fig. (6-2) shows the result for the initial 10 seconds when the synaptic weights have not been tuned to the precise values. Shown in the left two panels are the channel variables s_1 and s_2, while in the right two panels are the firing rates of these two neurons. After each saccade, the integrator neuron can not hold persistent activities, but the drift is becoming smaller as the learning continues.

We also plot the result of the last 10 seconds in Fig. (6-3). The same as in Fig. (6-2), shown the left two panels are channel variables s_1 and s_2 and in the right are firing rates. Compared with Fig. (6-2) the drift during gaze-holding period is much smaller indicating the learning of stabilization.

In Fig. (6-4) we show the change of the tonic and recurrent weights during the whole learning period.

We also plot the firing rate of one neuron as a function of the other neuron in the

state space in Fig. (6-5). Consistent well with Eq. (6.11), it forms a line in the state space.

6.2 Recurrent network with five memory neurons

We have shown that the learning in the coupled network performs quite well for stabilizing the persistent neural activity. Next we will implement the learning rule in a more complicated network with 5 memory neurons.

The network is run for 100 seconds with the learning rules implemented. The saccade is initiated randomly for every 500 ms. The parameters on the tonic and burst neurons are the same as those in the coupled neurons. The synaptic weights for the recurrent and tonic synapses are first calculated using the method of tuning introduced in Chapter 3, and then corrupted with noise.

Fig. (6-6) shows the simulation results in three panels taken from three different time period. Shown in each panel is the channel variable of burst excitatory neuron, burst inhibitory neuron and five memory neurons respectively. The top panel is taken from the first 10 seconds of simulation. since the weights are not tuned, all five neurons can not hold persistent neural activity after each saccade. All s quickly decay to zero.

The result in 10 - 20 seconds are shown in the middle panel. Memory neurons start to be able to keep persistent activity thought drift is high.

We also taken the simulation result in the last 10 seconds of learning period and shown it in the last panel of Fig. (6-6). The network's ability to hold persistent activity during gaze holding period is fairly well at this time domain.

In Fig. (6-4) we show the change of the tonic and recurrent weights during the whole learning period.

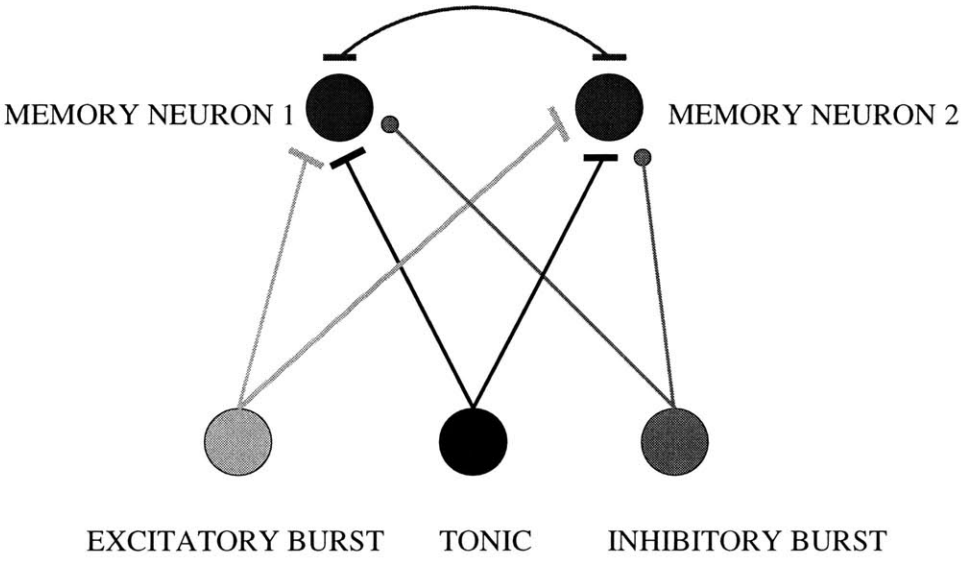

Figure 6-1: Diagram of coupled neuron model

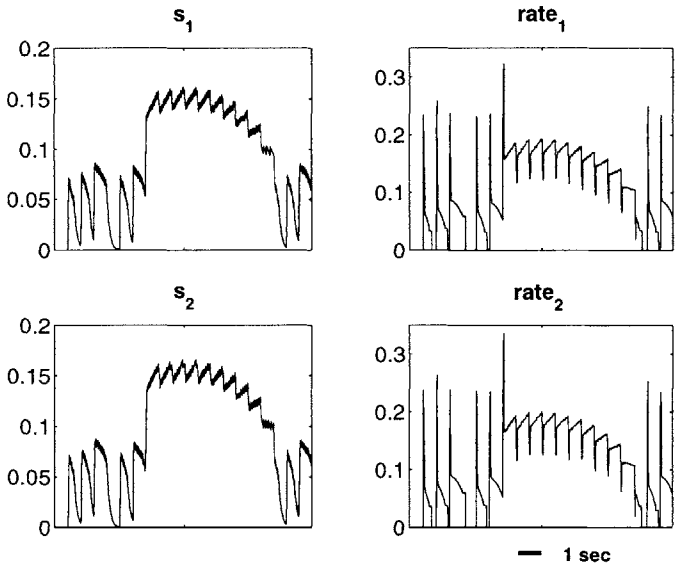

Figure 6-2: Positively coupled integrator neurons with untuned weights. This figure shows the result for the initial 10 seconds when the synaptic weights have not been tuned to the precise values. Shown in the left two panels are the channel variables s_1 and s_2, while in the right two panels are the firing rates of these two neurons. After each saccade, the integrator neuron can not hold persistent activities, but the drift is becoming smaller as the learning continues.

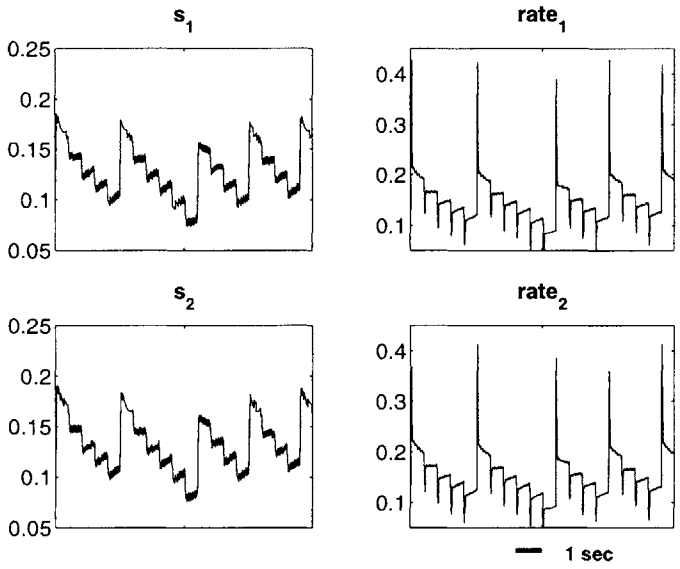

Figure 6-3: Positively coupled integrator neurons with learning. This figure shows the result for the last 10 seconds of learning. Shown in the left two panels are the channel variables s_1 and s_2, while in the right two panels are the firing rates of these two neurons. Compared with Fig. (6-2) the drift during gaze-holding period is much smaller indicating the learning of stabilization.

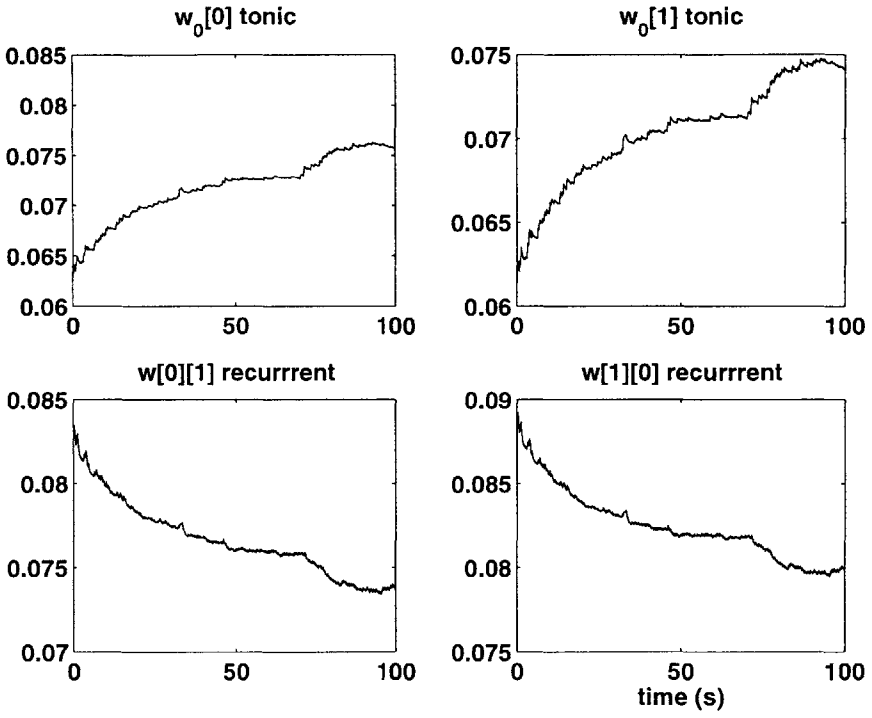

Figure 6-4: The change of synaptic weights during the learning period of 100 seconds. Shown in the top two panels are the tonic synaptic weights. In the bottom is the recurrent weights.

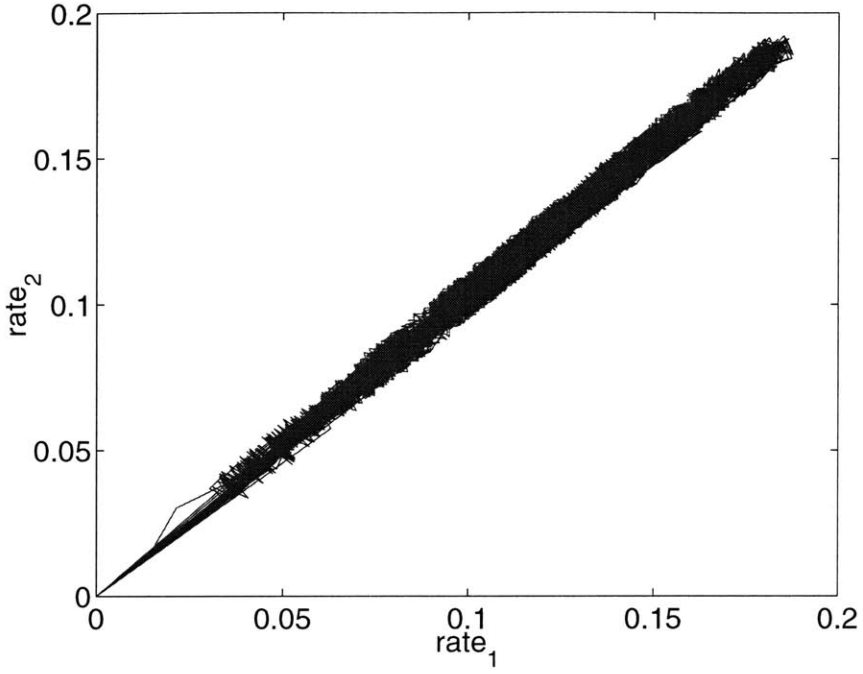

Figure 6-5: The firing rate of one neuron plotted as a function of the firing rate of the other neuron. In the state space, it forms a line.

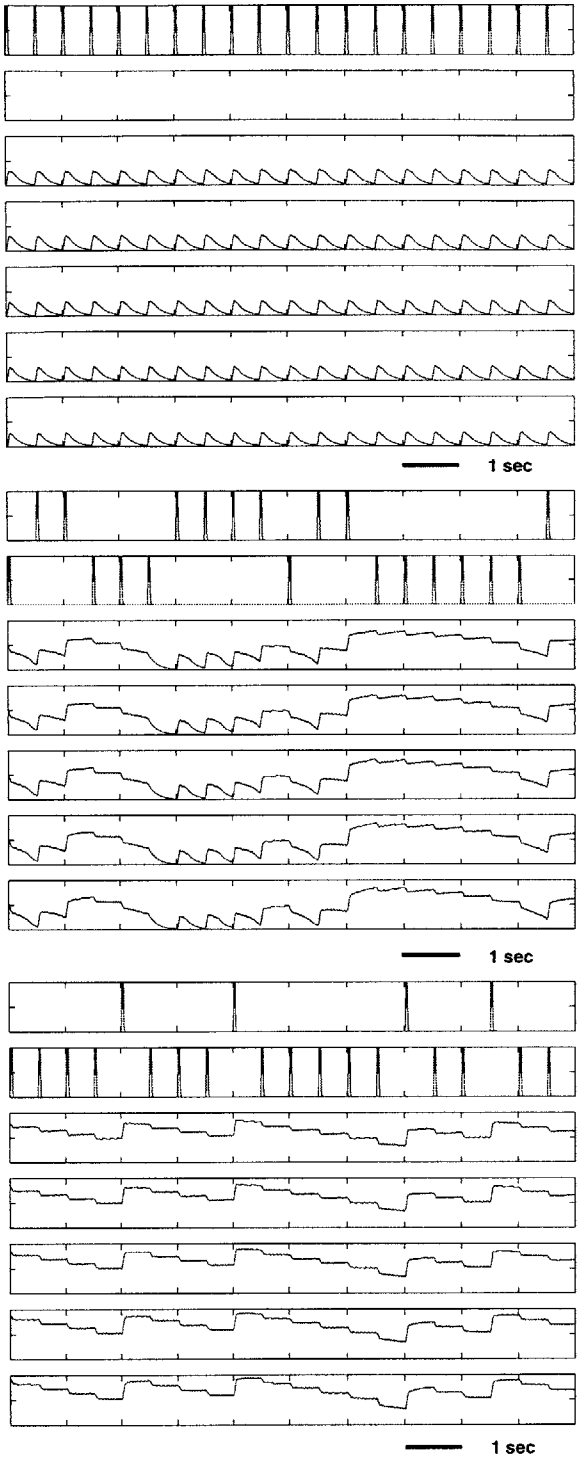

Figure 6-6: Five recurrent integrator neurons with learning. This figure shows the simulation results in three panels taken from first 10 seconds, 10-20 seconds and the last 10 seconds respectively. In each panel shown is the channel variable of burst excitatory neuron, burst inhibitory neuron and five memory neurons respectively.

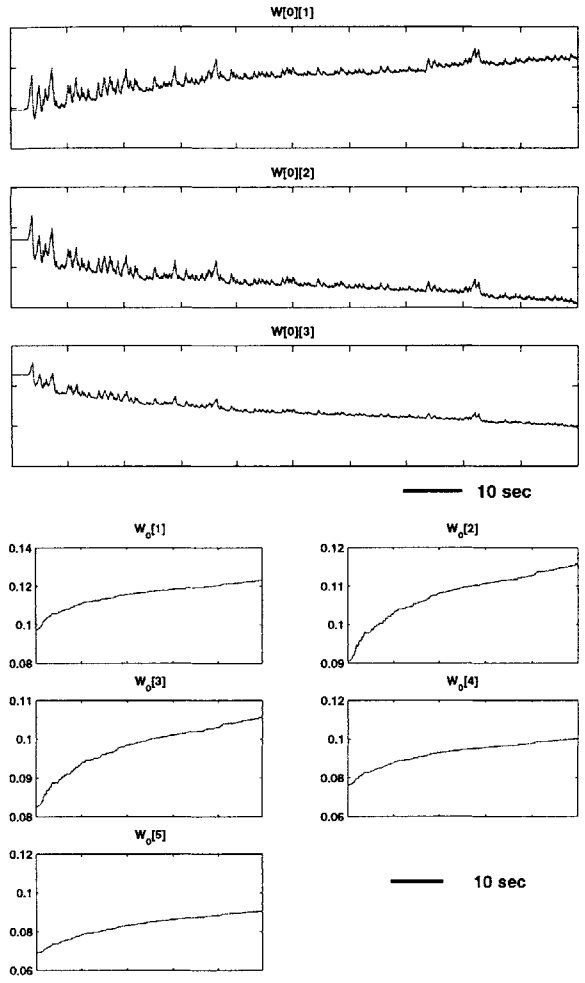

Figure 6-7: The synaptic weight during the learning. Shown in the top five panels is the tonic synaptic weights. In the bottom three panels are three selected recurrent synaptic weights.

Chapter 7

Conclusion

In this thesis, we have studied a biophysically plausible mechanism for the function of the occulomotor neural integrator, a premotor area responsible for controlling the eye movement. In the saccadic eye movement, a transient input causes a step change in the activity of the integrator neuron, and the elevated or suppressed activity could sustain for up to many seconds. This persistent neural activity is said to hold a short term memory of the eye position. To keep the eye still, the drift in the neural activity of the integrator neuron during the gaze-holding period has to be very low. In this thesis, we have proposed a recurrent neural network model for the function of the neural integrator.

The recurrent neural network is composed of the integrator-and-fire neurons which are connected with each other. By using the method of averaging, we are able to reduce this spike-based model into a network model with continuous variables in the Wilson-Cowan form.

We illustrated on how to tune the synaptic weights of the autapse and the network model such that the fixed points of the neural dynamics will approximately form a line attractor in the state space. Throughout the thesis, we have argued that it is this line attractor that forms the basis of the short term memory at different continuous values.

The tuned feedback model has been criticized as unrobust because it requires precise tuning of the synaptic weights. The question on how to tune and adaptively

control the synaptic weights are addressed in Chapters 4-6. We have proposed a spike-based learning rule to adaptively tune the synaptic weights.

The spike-based learning rule depends critically on the temporal differences of the pre and post spikes. According to this rule, a synapse depresses when a presynaptic spike is followed by a postsynaptic spike, and potentiates when the order is reversed. We then showed that this spike-based learning rule could be reduced to rate-based one under certain conditions. We found that this learning rule acts as a gradient descend method for minimizing the drift of the neural activity during gaze-holding period.

The spike-based learning rules have been implemented in both an autapse model with localized feedback and recurrent network model with distributed feedback. The simulation results of these models have shown that the spike-based differential anti-Hebbian learning rules are very effective in reducing the drift, which is consistent with our analysis in the continuous rate model.

Bibliography

[1] H. S. Seung, D. D. Lee, B. Y. Reis, and D. W. Tank. Stability of the memory of eye position in a recurrent network of conductance-based model neurons. *Neuron*, 26:259–71, 2000.

[2] D. A. Robinson. Integrating with neurons. *Annu Rev Neurosci*, 12:33–45, 1989.

[3] S. C. Cannon, D. A. Robinson, and S. Shamma. A proposed neural network for the integrator of the oculomotor system. *Biol. Cybern.*, 49:127–136, 1983.

[4] K. Zhang. Representation of spatial orientation by the intrinsic dynamics of the head-direction cell ensemble: a theory. *J Neurosci*, 16:2112–26, 1996.

[5] J. M. Fuster. Memory in the cortex of the primate. *Biol Res*, 28:59–72, 1995.

[6] R. Desimone. Neural mechanisms for visual memory and their role in attention. *Proc Natl Acad Sci U S A*, 93:13494–9, 1996.

[7] D. B. Arnold and D. A. Robinson. The oculomotor integrator: testing of a neural network model. *Exp Brain Res*, 113:57–74, 1997.

[8] A. K. Moschovakis. The neural integrators of the mammalian saccadic system. *Front Biosci*, 16:D552–D577, 1997.

[9] J. Yokota, H. Reisine, and B. Cohen. Nystagmus induced by electrical stimulation of the vestibular and prepositus hypoglossi nuclei in the monkey: evidence for site of induction of velocity storage. *Exp Brain Res*, 92:123–38, 1992.

[10] S. C. Cannon and D. A. Robinson. Loss of the neural integrator of the oculomotor system from brain stem lesions in monkey. *J Neurophysiol*, 57:1383–409, 1987.

[11] A. M. Pastor, B. Torres, J. M. Delgado-Garcia, and R. Baker. Discharge characteristics of medial rectus and abducens motoneurons in the goldfish. *J Neurophysiol*, 66:2125–40, 1991.

[12] A. M. Pastor, l. a. De, and R. Baker. Eye position and eye velocity integrators reside in separate brainstem nuclei. *Proc Natl Acad Sci U S A*, 91:807–11, 1994.

[13] L. Shen. Neural integration by short term potentiation. *Biol Cybern*, 61:319–25, 1989.

[14] J. E. Lisman, J. M. Fellous, and X. J. Wang. A role for nmda-receptor channels in working memory. *Nat Neurosci*, 61:273–5, 1998.

[15] R. H. Lee and C. J. Heckman. Bistability in spinal motoneurons in vivo: systematic variations in rhythmic firing patterns. *J Neurophysiol*, 80:572–82, 1998.

[16] M. B. Feller, K. R. Delaney, and D. W. Tank. Presynaptic calcium dynamics at the frog retinotectal synapse. *J Neurophysiol*, 76:381–400, 1996.

[17] F. Lorente de Nó. Vestibulo-ocular reflex arc. *Arch. Neurol. Psych.*, 30:245–291, 1933.

[18] D. J. Amit. The hebbian paradigm reintegrated: local reverberations as internal representations. *Behav Brain Sci*, 18:617–626, 1995.

[19] J. J. Hopfield. Neural networks and physical systems with emergent collective computational abilities. *Proc. Nat. Acad. Sci. USA*, 79:2554–2558, 1982.

[20] J. J. Hopfield. Neurons with graded response have collective computational properties like those of two-state neurons. *Proc. Natl. Acad. Sci. USA*, 81:3088–3092, 1984.

[21] D. B. Arnold and D. A. Robinson. A learning network model of the neural integrator of the oculomotor system. *Biol. Cybern.*, 64:447–454, 1991.

[22] H. Collewijn. Optokinetic and vestibulo-ocular reflexes in dark-reared rabbits. *Exp Brain Res*, 27:287–300, 1977.

[23] D. O. Hebb. *Organization of behavior.* Wiley, New York, 1949.

[24] C. C. Bell, H. Z. Han, Y Sugawara, and K. Grant. Synaptic plasticity in a cerebellum-like structure depends on temporal order. *Nature*, 387:278–81, 1997.

[25] H. Markram, J. Lubke, M. Frotscher, and B. Sakmann. Regulation of synaptic efficacy by coincidence of postsynaptic aps and epsps. *Science*, 275(5297):213–5, 1997.

[26] G. Q. Bi and M. M. Poo. Synaptic modifications in cultured hippocampal neurons: dependence on spike timing, synaptic strength, and postsynaptic cell type. *J Neurosci*, 18(24):10464–72, 1998.

[27] H. R. Wilson and J. D. Cowan. A mathematical theory of the functional dynamics of cortical and thalamic nervous tissue. *Kybernetik*, 13:55–80, 1973.

[28] H. R. Wilson and J. D. Cowan. Excitatory and inhibitory interactions in localized populations of model neurons. *Biophys J.*, 12:1–24, 1972.

[29] X. J. Wang. Synaptic basis of cortical persistent activity: the importance of nmda receptors to working memory. *J Neurosci*, 19(21):9587–603, 1999.

[30] C. Koch and I. Segev. *Methods in Neuronal Modeling.* Computational Neuroscience. The MIT Press, Cambridge, 1998.

[31] W. Gerstner, R. Kempter, J. L. van Hemmen, and H. Wagner. A neuronal learning rule for sub-millisecond temporal coding. *Nature*, 383(6595):76–81, 1996.

[32] L. F. Abbott and S. Song. Temporally asymmetric hebbian learning, spike timing and neuronal response variability. *Adv. Neural Info. Proc. Syst.*, 11, 1999.

[33] H. S. Seung. Learning to integrate without visual feedback. *Soc. Neurosci. Abstr.*, 23(1):8, 1997.

[34] A. P. Georgopoulos, M. Taira, and A. Lukashin. Cognitive neurophysiology of the motor cortex. *Science*, 260:47–52, 1993.

[35] M. Camperi and X. J. Wang. A model of visuospatial working memory in prefrontal cortex: recurrent network and cellular bistability [in process citation]. *J Comput Neurosci*, 5(4):383–405, 1998.

[36] H. S. Seung. How the brain keeps the eyes still. *Proc. Natl. Acad. Sci. USA*, 93:13339–13344, 1996.

[37] B. Ermentrout. Reduction of conductance-based models with slow synapses to neural nets. *Neural Comput.*, 6:679–695, 1994.

[38] O. Shriki, H. Sompolinsky, and D. Hansel. Rate models for conductance based cortical neural networks. *preprint*, 1999.